TIDAL PRISM - INLET AREA RELATIONSHIPS

by

James T. Jarrett

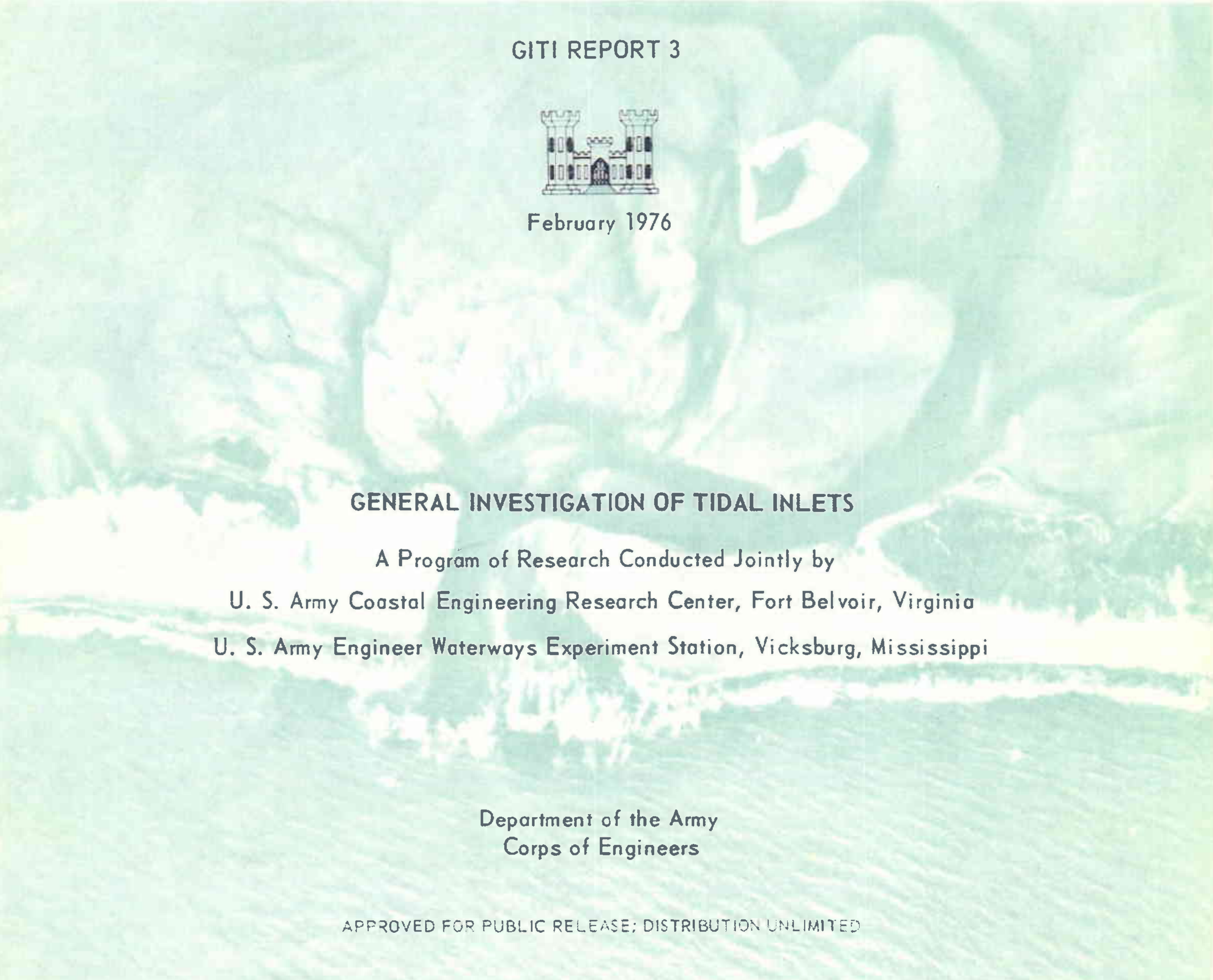

GITI REPORT 3

February 1976

GENERAL INVESTIGATION OF TIDAL INLETS

A Program of Research Conducted Jointly by

U. S. Army Coastal Engineering Research Center, Fort Belvoir, Virginia

U. S. Army Engineer Waterways Experiment Station, Vicksburg, Mississippi

Department of the Army
Corps of Engineers

Cover Photo: Drum Inlet, North Carolina, 13 March 1962
Courtesy of the U. S. Geological Survey

Unclassified

SECURITY CLASSIFICATION OF THIS PAGE (When Data Entered)

REPORT DOCUMENTATION PAGE		READ INSTRUCTIONS BEFORE COMPLETING FORM
1. REPORT NUMBER GITI Report 3	2. GOVT ACCESSION NO.	3. RECIPIENT'S CATALOG NUMBER
4. TITLE (and Subtitle) TIDAL PRISM - INLET AREA RELATIONSHIPS		5. TYPE OF REPORT & PERIOD COVERED Final report
		6. PERFORMING ORG. REPORT NUMBER
7. AUTHOR(s) James T. Jarrett		8. CONTRACT OR GRANT NUMBER(s)
9. PERFORMING ORGANIZATION NAME AND ADDRESS U. S. Army Engineer Waterways Experiment Station Hydraulics Laboratory P. O. Box 631, Vicksburg, Miss. 39180		10. PROGRAM ELEMENT, PROJECT, TASK AREA & WORK UNIT NUMBERS
11. CONTROLLING OFFICE NAME AND ADDRESS U. S. Army Coastal Engineering Research Center Kingman Building Fort Belvoir, Va. 22060		12. REPORT DATE February 1976
		13. NUMBER OF PAGES 55
14. MONITORING AGENCY NAME & ADDRESS(if different from Controlling Office)		15. SECURITY CLASS. (of this report) Unclassified
		15a. DECLASSIFICATION/DOWNGRADING SCHEDULE

16. DISTRIBUTION STATEMENT (of this Report)

Approved for public release; distribution unlimited.

17. DISTRIBUTION STATEMENT (of the abstract entered in Block 20, if different from Report)

18. SUPPLEMENTARY NOTES

19. KEY WORDS (Continue on reverse side if necessary and identify by block number)

Tidal inlets
Tidal prisms

20. ABSTRACT (Continue on reverse side if necessary and identify by block number)

The tidal prism - inlet area relationships for inlets on sandy coast established by M. P. O'Brien were reanalyzed using his data and data published by other investigators. In addition, tidal prism and inlet cross-sectional area data developed in the Inlet Classification Study, a subfeature of the Corps of Engineers General Investigation of Tidal Inlets, were also used. These data result in a total of 162 data points for 108 inlets--59 of which are located on the Atlantic coast, 24 on the Gulf coast, and 25 on the Pacific coast of
(Continued)

DD FORM 1473, 1 JAN 73 EDITION OF 1 NOV 65 IS OBSOLETE

Unclassified

SECURITY CLASSIFICATION OF THIS PAGE (When Data Entered)

20. ABSTRACT (Continued).

the United States. The data are grouped into three main categories, namely: (1) all inlets, (2) unjettied and single-jettied inlets, and (3) inlets with two jetties. Within each of these three categories, the data are further subdivided into: (a) inlets on all three coasts, (b) inlets on the Atlantic coast, (c) inlets on the Gulf coast, and (d) inlets on the Pacific coast. Regression analysis was performed on each set of data to determine the equations of best fit and to establish 95 percent confidence limits for the equations and the constants in the equations. The results of the regression analysis, which in all cases yielded an equation of the form $A = CP^n$, in which C and n are constants determined by the regression analysis, indicate that the tidal prism - inlet area relationship is not a unique function for all inlets but varies depending on inlet location and whether or not the inlet has been stabilized with a dual jetty system.

FOREWORD

This report was prepared by the Estuaries and Wave Dynamics Divisions of the Hydraulics Laboratory at the U. S. Army Engineer Waterways Experiment Station (WES) as one in a series of reports on the General Investigation of Tidal Inlets (GITI). The GITI research program is under the technical surveillance of the U. S. Army Coastal Engineering Research Center (CERC) and is conducted by CERC, WES, and other Government and private organizations. During the study of the Keulegan repletion coefficient being done as a part of the Inlet Classification Study, the opportunity was taken to make this reanalysis of the relationships between tidal prism and inlet area originally developed by M. P. O'Brien in 1931. Because the tidal prisms calculated to determine the repletion coefficient for tidal inlets also provide additional data on the relationship between tidal prism and inlet area, advantage was taken of the new data to investigate its effect on the previously developed relationships.

The study and report preparation were supervised by E. C. McNair (former WES GITI Program Manager), CPT F. C. Perry, CE (present WES GITI Program Manager), R. A. Sager, Chief of the Estuaries Division, R. W. Whalin, Chief of the Wave Dynamics Division, and H. B. Simmons, Chief of the Hydraulics Laboratory. Civilian members of the Coastal Engineering Research Board, Dean Morrough P. O'Brien, Professor Robert G. Dean, Professor Robert L. Wiegel, and Professor Arthur T. Ippen (former member, deceased), were intimately involved in both the planning and review of this report. CERC technical direction was conducted by C. Mason and R. M. Sorensen. Technical Directors of CERC and WES were T. Saville, Jr., and F. R. Brown, respectively.

Comments on this publication are invited.

Approval for publication in accordance with Public Law 166, 79th Congress, approved 31 July 1945, as supplemented by Public Law 172, 88th Congress, approved 7 November 1963:

G. H. HILT
Colonel, Corps of Engineers
Director
Waterways Experiment Station

JAMES L. TRAYERS
Colonel, Corps of Engineers
Commander and Director
Coastal Engineering Research Center

PREFACE

1. The Corps of Engineers, through its Civil Works program, has sponsored, over the past twenty-three years, research into the behavior and characteristics of tidal inlets. The Corps' interest in tidal inlet research stems from its responsibilities for navigation, beach erosion prevention and control, and flood control. Tasked with the creation and maintenance of navigable U. S. waterways, the Corps routinely dredges millions of cubic yards of material each year from tidal inlets that connect the ocean with bays, estuaries, and lagoons. Design and construction of navigation improvements to existing tidal inlets are an important part of the work of many Corps offices. In some cases, design and construction of new inlets are required. Development of information concerning the hydraulic characteristics of inlets is important not only for navigation and inlet stability but also because inlets control the daily exchange of water between bay and ocean. Accurate predictions of the effects of storm surges and runoff also require an understanding of inlet hydraulics during extreme conditions.

2. A research program, the General Investigation of Tidal Inlets program, was developed to provide quantitative data for use in design of inlets and inlet improvements. It is designed to meet the following objectives:

> To determine the effects of wave action, tidal flow, and related phenomena on inlet stability and on the hydraulic, geometric, and sedimentary characteristics of tidal inlets; to develop the knowledge necessary to design effective navigation improvements, new inlets, and sand transfer systems at existing tidal inlets; to evaluate the water transfer and flushing capability of tidal inlets; and to define the processes controlling inlet stability.

3. The GITI is divided into three major study areas: inlet classification, inlet hydraulics, and inlet dynamics.

- a. The objectives of the inlet classification study are to classify inlets according to their geometry, hydraulics, and stability, and to determine the relationships that exist among the geometric and dynamic characteristics and the environmental factors that control these characteristics. The classification study keeps the general investigation closely related to real inlets and produces an important inlet data base useful in documenting the characteristics of inlets.

b. The objectives of the inlet hydraulics study are to define the tide-generated flow regime and water-level fluctuations in the vicinity of coastal inlets and to develop techniques for predicting these phenomena. The inlet hydraulics study is divided into three areas: idealized inlet model study, evaluation of state-of-the-art physical and numerical models, and prototype inlet hydraulics.

(1) The idealized inlet model. The objectives of this model study are to determine the effect of inlet configurations and structures on discharge, head loss, and velocity distribution for a number of realistic inlet shapes and tide conditions. An initial set of tests in a trapezoidal inlet was conducted between 1967 and 1970. However, in order that subsequent inlet models are more representative of real inlets, a number of "idealized" models representing various inlet morphological classes are being developed and tested. The effects of jetties and wave action on the hydraulics are included in the study.

(2) Evaluation of state-of-the-art modeling techniques. The objectives of this portion of the inlet hydraulics study are to determine the usefulness and reliability of existing physical and numerical modeling techniques in predicting the hydraulic characteristics of inlet/bay systems, and to determine whether simple tests, performed rapidly and economically, are useful in the evaluation of proposed inlet improvements. Masonboro Inlet, N. C., was selected as the prototype inlet which would be used along with hydraulic and numerical models in the evaluation of existing techniques. In September 1969 a complete set of hydraulic and bathymetric data was collected at Masonboro Inlet. Construction of the fixed-bed physical model was initiated in 1969, and extensive tests have been performed since then. In addition, three existing numerical models were applied to predict the inlet's hydraulics. Extensive field data were collected at Masonboro Inlet in August 1974 for use in evaluating the capabilities of the physical and numerical models.

(3) Prototype inlet hydraulics. Field studies at a number of inlets are providing information on prototype inlet/bay tidal hydraulic relationships and the effects of friction, waves, tides, and inlet morphology on these relationships.

c. The basic objective of the inlet dynamics study is to investigate the interactions of tidal flow, inlet configuration, and wave action at tidal inlets as a guide to improvement of inlet channels and nearby shore protection works. The study is subdivided into four specific areas: model materials evaluation, movable-bed modeling evaluation, reanalysis of a previous inlet model study, and prototype inlet studies.

(1) Model materials evaluation. This evaluation was initiated in 1969 to provide data on the response of movable-bed model materials to waves and flow to allow selection of the optimum bed materials for inlet models.

(2) Movable-bed model evaluation. The objective of this study is to evaluate the state-of-the-art of modeling techniques, in this case movable-bed inlet modeling. Since, in many cases, movable-bed modeling is the only tool available for predicting the response of an inlet to improvements, the capabilities and limitations of these models must be established.

(3) Reanalysis of an earlier inlet model study. In 1957, a report entitled "Preliminary Report: Laboratory Study of the Effect of an Uncontrolled Inlet on the Adjacent Beaches" was published by the Beach Erosion Board (now CERC). A reanalysis of the original data is being performed to aid in planning of additional GITI efforts.

(4) Prototype dynamics. Field and office studies of a number of inlets are providing information on the effects of physical forces and artificial improvements on inlet morphology. Of particular importance are studies to define the mechanisms of natural sand bypassing at inlets, the response of inlet navigation channels to dredging and natural forces, and the effects of inlets on adjacent beaches.

4. This report is a secondary result of the research being conducted as part of the inlet classification study. During a study of the variation in the Keulegan repletion coefficient (K) with variations in inlet geomorphology as a means of classifying inlets (report in preparation), a great deal of new tidal prism data was generated during the calculation of Keulegan's K for many inlets. The opportunity was therefore taken to reexamine the relationships between tidal prism and inlet area which were originally developed by M. P. O'Brien in 1931.

CONTENTS

CONVERSION FACTORS, U. S. CUSTOMARY TO METRIC (SI) UNITS OF MEASUREMENT

U. S. customary units of measurement used in this report can be converted to metric (SI) units as follows:

Multiply	By	To Obtain
feet	0.3048	metres
square feet	0.0929	square metres
cubic feet	0.0283	cubic metres
feet per second	0.3048	metres per second

TIDAL PRISM - INLET AREA RELATIONSHIPS

PART I: INTRODUCTION

1. The first known published relationship between the cross-sectional area of a tidal inlet and the tidal prism were given by L. J. LeConte[1] in 1905 for harbor entrances on the Pacific coast. Using standard notation, LeConte's relationship can be expressed as:

$$A = 3.3 \times 10^{-5} P \quad \text{for unprotected entrances} \tag{1}$$

and

$$A = 4.3 \times 10^{-5} P \quad \text{for inner harbor entrances} \tag{2}$$

where

A = gorge cross-sectional area below mean sea level (msl), sq ft*

P = tidal prism corresponding to the spring range of tide, cu ft

LeConte cited conditions at the harbor entrances at San Diego, San Pedro, San Francisco, and Humboldt, Calif., as fitting Equation 1.

2. In 1931, M. P. O'Brien[2] established a relationship between the cross-sectional area of an inlet and its tidal prism. This relationship, based primarily on data pertaining to Pacific coast inlets, was

$$A = 4.69 \times 10^{-4} P^{0.85} \tag{3}$$

where

A = minimum cross section of entrance channel measured below msl, sq ft

P = tidal prism corresponding to the diurnal or spring range of tide, cu ft

In 1969, O'Brien[3] reviewed this relationship in the light of additional data that had become available since the initial study. Included in

---

* For convenience, symbols and unusual abbreviations are listed and defined in the Notation (Appendix A). A table of factors for converting U. S. customary units of measurement to metric (SI) units is presented on page 6.

this review were data for 28 inlets, 9 on the Atlantic coast, 18 on the Pacific coast, and 1 on the Gulf coast. O'Brien concluded from this review that the original relationship agreed closely with the contemporary data for inlets with two jetties but that inlets without jetties appeared to be better represented by the linear relationship

$$A = 2.0 \times 10^{-5} P \qquad (4)$$

3. In 1971 I. V. Nayak[4] investigated the relationship between the tidal prism and the cross-sectional area in a model inlet. Two series of tests were conducted with the model inlet, namely: (a) no jetties without waves and with waves, and (b) twin jetties without waves and with waves. From the results of his experiments, experiments conducted at the University of Florida,[5] and available prototype data, Nayak concluded that the tidal prism - inlet area relationship for jettied inlets could be approximated by

$$\frac{P}{A} = 2.4 \times 10^{3} P^{0.15} \qquad (5)$$

or rearranging

$$A = 4.17 \times 10^{-4} P^{0.85} \qquad (6)$$

For unjettied inlets, the only suitable relationship appeared to be $P/A = 5.3 \times 10^{4}$ or

$$A = 1.89 \times 10^{-5} P \qquad (7)$$

Although these relationships agree closely with those developed by O'Brien, the primary source of prototype data used by Nayak was O'Brien.[3] In addition, from the test conducted with the unjettied inlet and no waves, Nayak observed that the size of the cross-sectional area which developed agreed closely with that produced in the test with the jettied inlet. Also, for the test with the unjettied inlet with waves, long-period waves produced smaller minimum cross-sectional areas than did short-period waves.

4. J. W. Johnson,[6] working with inlets on the Pacific coast, used hydrographic surveys available from the Corps of Engineers and National Ocean Survey (formerly USC&GS) navigation charts to measure entrance areas and bay surface areas. Mean and diurnal tidal prisms were calculated by multiplying the bay surface area by the mean and diurnal tide ranges near the inlet entrance. From his plot of mean tidal prism (P_m) against cross-sectional area for all inlets, Johnson arrived at the relationship

$$P_m = 9 \times 10^3 A^{1.13} \quad (8)$$

or rearranging

$$A = 3.17 \times 10^{-4} P_m^{0.88} \quad (9)$$

When he extended the data to include laboratory data from the University of Florida[5] and the University of California,[4,7] the resulting equation was

$$\frac{P_m}{A} = 5 \times 10^3 P^{0.10} \quad (10)$$

Again rearranging

$$A = 2.0 \times 10^{-4} P_m^{0.90} \quad (11)$$

For six unimproved inlets, Johnson simply averaged the P_m/A values for these inlets and found

$$\frac{P_m}{A} = 5.5 \times 10^4 \quad (12)$$

or

$$A = 1.82 \times 10^{-5} P_m \qquad (13)$$

which is similar to the results of both O'Brien and Nayak.

5. The majority of the prototype data used by these investigators were for Pacific coast inlets, most of which had been stabilized with dual jetty systems. This report attempts to determine if inlets on all three coasts of the United States follow the same tidal prism - inlet area relationship, and also to establish what effect inlet stabilization has on this relationship.

PART II: TIDAL PRISM - INLET AREA DATA USED IN THE ANALYSIS

6. Table 1 lists all of the tidal prism - inlet area data used for this study and its source. A total of 162 data points are given in this table for 108 inlets. Of the 108 inlets, 59 are located on the Atlantic coast, 24 on the Gulf coast, and 25 on the Pacific coast. Of the 162 data points, 92 are attributable to data published by other investigators or are taken from Corps of Engineers prototype flow measurements, whereas the remaining 70 data points, which are limited to the Atlantic and Gulf coasts, are the result of computations made in connection with the Inlet Classification Study at the WES. Two computational methods have been employed to compute these additional 70 tidal prisms, one designated as the "cubature method" and the other as the "NOS current data method." An explanation of these two methods follows.

Cubature Method

7. The cubature method for calculating tidal prisms takes into account the time required for a tidal wave to propagate through the inlet and into the bay, i.e., rather than assuming a uniform rise and fall of the tide over the entire bay, the cubature method segments the bay into subareas that have approximately the same "phase range." Phase range is defined as the difference between the water-surface elevation at a particular point in the bay at the time of a slack water in the inlet (say, slack--flood begins) and the elevation at that same point at the time of a subsequent slack water in the inlet (say, slack--ebb begins). In other words, the phase range is the absolute difference in water-surface elevation at a point in the bay that occurs during the time water is either flowing into or out of an inlet. In order to arrive at the phase range for various bays, the tide prediction information contained in the National Ocean Survey (NOS) Tide Tables[8] was used. Tide prediction stations were grouped according to their applicability to a particular inlet-bay system and the tidal amplitude for each tide

prediction station was tabulated along with the average time corrections for high and low water relative to a reference station. Using an average ocean tide period of 12 hr and 25 min for a semidiurnal tide (Atlantic coast) and 24 hr and 50 min for a diurnal tide (Gulf coast) and assuming a sinusoidal variation of the ocean tide, average tide curves were prepared for each tide prediction station. The Fire Island inlet-bay system is used to illustrate this method. Although the phase difference between bay tide stations is not large, this inlet was selected because of the comprehensive tidal data available. A set of average tide curves for the inlet-bay system is shown in Figure 1. The location of each of these tide prediction stations for this inlet is shown in Figure 2. For most inlets, a tide prediction station is located in the entrance or just bayward of the entrance (sta 70 for Fire Island Inlet). Using the average tide curve for this inlet station and the average tide curve for the ocean station nearest the inlet, slack water in the inlet was taken as the time when the ocean tide curve crossed the inlet tide curve. If tidal current tables are available, the time of slack water can be obtained directly from the tables. The time interval between two succeeding slack waters represents the time during which water flows through the inlet. With slack water in the inlet thus determined, the surface elevation at each bay tide prediction station was read from the average tide curves for the times of two subsequent slack waters; the difference between these two elevations for a particular station represents its phase range. This procedure is indicated in Figure 1, which gives a tabulation of the two slack-water elevations and the resulting phase range for the various tide stations. After determining the phase range for each station, the bay was contoured into subareas of approximately the same phase range (Figure 2) and the average surface area of the subareas was calculated as the mean of the high and low water-surface areas. The average surface area of each subarea was then multiplied by the phase range of that subarea to yield the volume of water entering (or leaving) the subarea during the interval of time between succeeding slack waters in the inlet. The total volume of water entering (or leaving) the bay, which is the tidal prism, was then computed by

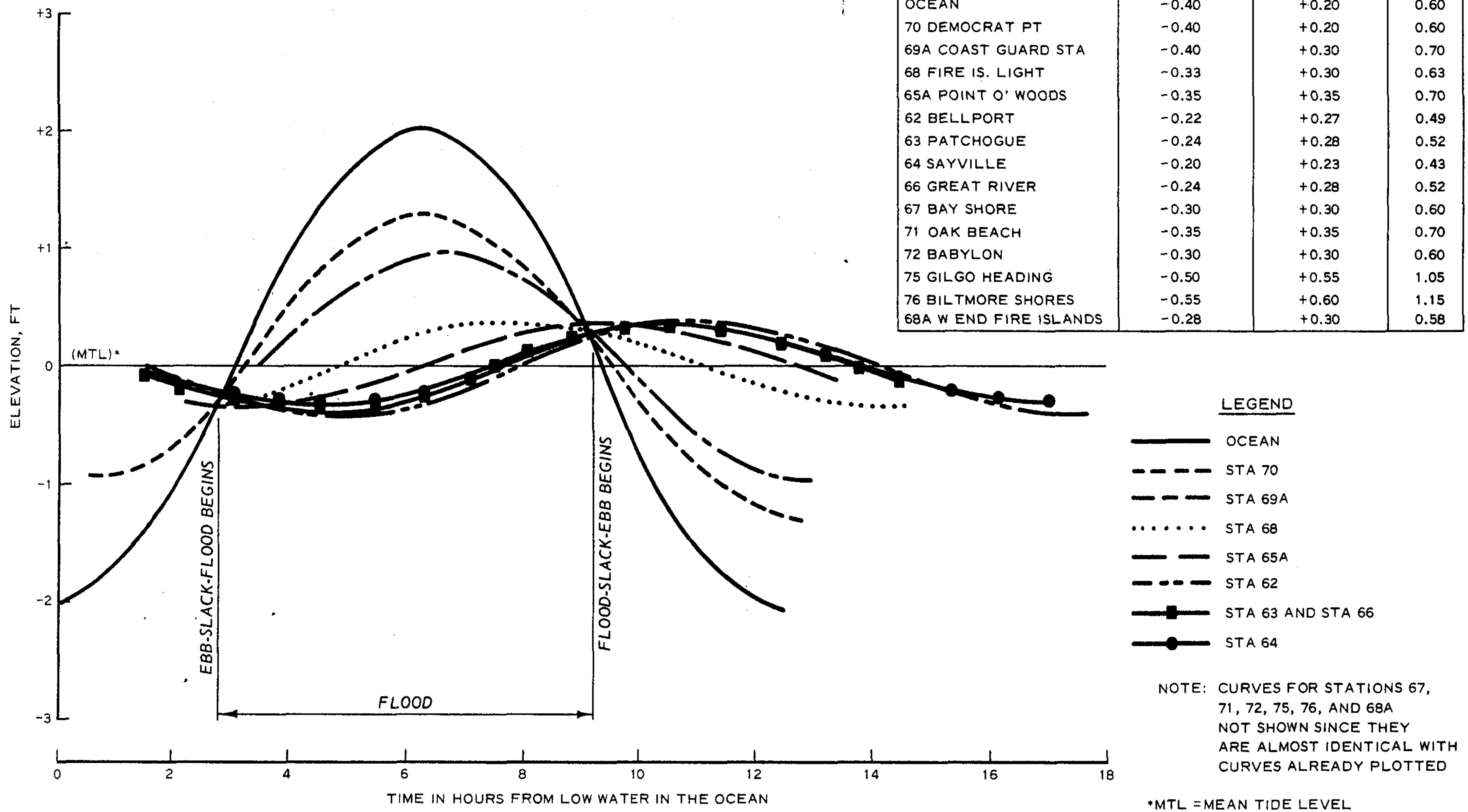

TABLE OF PHASE RANGES

STATION	EL AT EBB-SLACK-FLOOD BEGINS	EL AT FLOOD-SLACK-EBB BEGINS	PHASE RANGE FT
OCEAN	-0.40	+0.20	0.60
70 DEMOCRAT PT	-0.40	+0.20	0.60
69A COAST GUARD STA	-0.40	+0.30	0.70
68 FIRE IS. LIGHT	-0.33	+0.30	0.63
65A POINT O' WOODS	-0.35	+0.35	0.70
62 BELLPORT	-0.22	+0.27	0.49
63 PATCHOGUE	-0.24	+0.28	0.52
64 SAYVILLE	-0.20	+0.23	0.43
66 GREAT RIVER	-0.24	+0.28	0.52
67 BAY SHORE	-0.30	+0.30	0.60
71 OAK BEACH	-0.35	+0.35	0.70
72 BABYLON	-0.30	+0.30	0.60
75 GILGO HEADING	-0.50	+0.55	1.05
76 BILTMORE SHORES	-0.55	+0.60	1.15
68A W END FIRE ISLANDS	-0.28	+0.30	0.58

Figure 1. Average tide curves for Fire Island Inlet and Great South Bay, New York

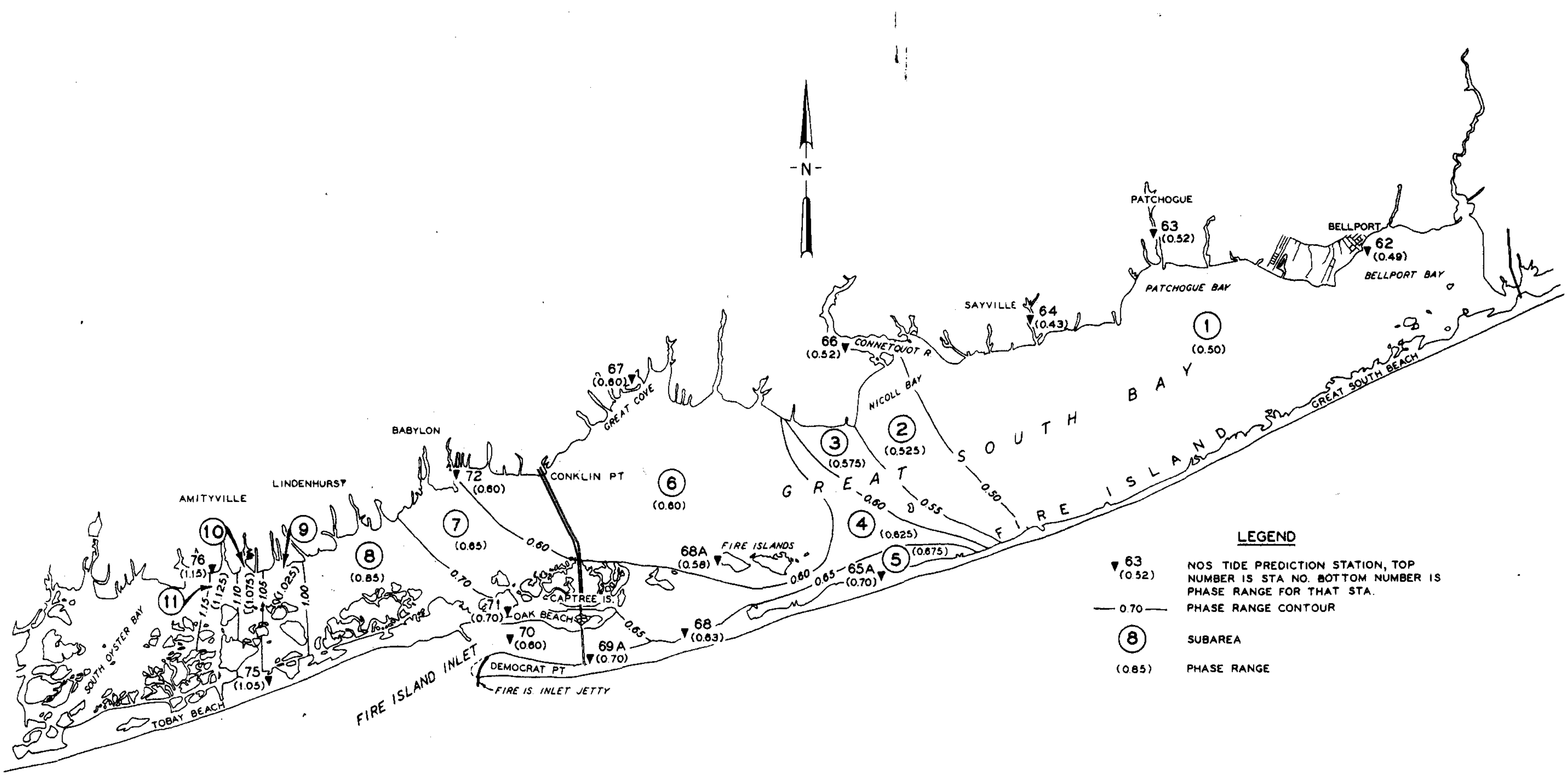

Figure 2. Fire Island Inlet-Great South Bay location of NOS tide prediction stations

summing the volume change of each subarea.

8. In relating the tidal prism computed by the cubature method to a minimum cross-sectional area, the inlet cross-sectional area was measured from NOS hydrographic surveys corresponding to the dates of tidal observations used to determine the tide prediction constants and differences contained in the Tide Tables. This is a necessary prerequisite, because these constants and differences are a function of the conditions existing at the bay entrance when the tides were observed. In all instances, the cross-sectional area was measured at the narrowest point in the inlet. Although the narrowest point in the inlet is not always the location of the minimum cross section, in most cases it closely coincides. A total of 39 tidal prisms and inlet areas, shown in Table 1, were computed by the cubature method.

NOS Current Data Method

9. Tidal current velocity observations made by the NOS in 31 inlets were used to compute tidal prisms for these inlets as shown in Table 1. These current observations were generally made at one vertical station near the throat of the inlet and consisted of continuous observations during one or more tidal cycles. Where possible, current observations made during spring tides were used to compute tidal prisms. If observations were not available for spring tide conditions, the spring tidal prism was estimated by a ratio of the bay tidal range during spring conditions to the bay tidal range at the time of the current observations. The inlet cross-sectional areas at the current measurement stations were obtained from NOS hydrographic surveys made at approximately the same time that the velocities were observed. Since the current measurement stations were located near the deepest part of the inlet where the velocities are usually greater than those through other parts of the cross section, a systematic procedure was established to reduce the observed velocities to a velocity that would be more representative of the average velocity through the entire cross section. This was accomplished by assuming that the velocity through the inlet

could be represented by Manning's equation:

$$V = \frac{1.49}{n} R^{2/3} S_e^{1/2} \tag{14}$$

where

n = friction coefficient

R = hydraulic radius

S_e = energy gradient

Although the frictional resistance (n) varies over the cross section, for these computations n was assumed to be constant for the entire cross section; also, the variation in the energy gradient across the cross section, S_e , was neglected. Under these assumptions, the variation in velocity from one portion of the cross section to another can be related by

$$\frac{V_1}{V_2} = \frac{R_1^{2/3}}{R_2^{2/3}} \tag{15}$$

where

V_1, V_2 = velocities associated with flow segments 1 and 2, respectively

R_1, R_2 = hydraulic radii

For those inlets that have a fairly simple cross section, the average velocity through the entire cross section was computed as

$$\frac{V_{avg}}{V_{meas}} = \frac{R^{2/3}}{D^{2/3}} \tag{16}$$

where

V_{avg} = average velocity over the entire cross section

V_{meas} = observed velocity at the one vertical section

R = hydraulic radius of the entire cross section

D = depth of water at the current meter location

10. For cross sections that were not of simple shape, the cross section was divided into several smaller flow sections depending upon

the complexity of the cross-sectional shape, and the hydraulic radius of each section was determined. The average velocity through the section in which the velocity meters were located (Section 1) was computed by

$$\frac{V_{1_{avg}}}{V_{meas}} = \frac{R_1^{2/3}}{D^{2/3}} \tag{17}$$

where

$V_{1_{avg}}$ = average velocity through Section 1

R_1 = hydraulic radius of Section 1

The average velocities through the other sections were then computed by Equation 15. An example of the above procedure is shown in Figure 3 for the cross section at the current gaging station at the entrance to Pensacola Bay.

11. By using the above procedure, average velocities were calculated at 1-hr increments during the tidal cycle. Discharges were calculated over the entire tidal cycle by adjusting the area of the flow cross section for fluctuations in tidal elevation. The discharges for ebb and flood flows were numerically integrated separately and then averaged to determine the tidal prism.

12. As for the cubature method, the minimum cross-sectional area associated with the tidal prism computed from the NOS current data was obtained at the narrow point in the inlet from surveys conducted by NOS at approximately the same time that the current measurements were taken.

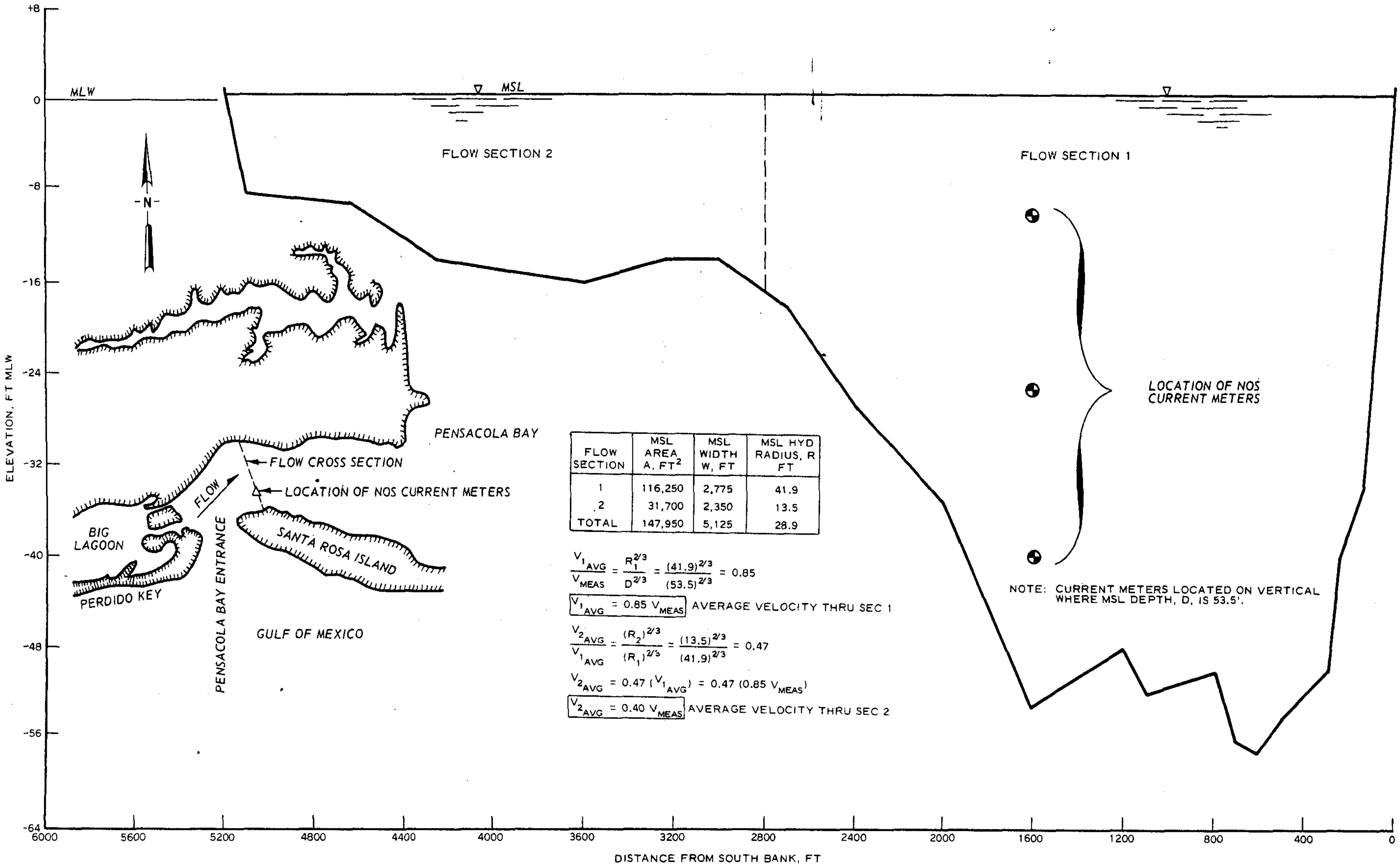

FLOW SECTION	MSL AREA A, FT^2	MSL WIDTH W, FT	MSL HYD RADIUS, R FT
1	116,250	2,775	41.9
2	31,700	2,350	13.5
TOTAL	147,950	5,125	28.9

$$\frac{V_{1_{AVG}}}{V_{MEAS}} = \frac{R_1^{2/3}}{D^{2/3}} = \frac{(41.9)^{2/3}}{(53.5)^{2/3}} = 0.85$$

$\boxed{V_{1_{AVG}} = 0.85\ V_{MEAS}}$ AVERAGE VELOCITY THRU SEC 1

$$\frac{V_{2_{AVG}}}{V_{1_{AVG}}} = \frac{(R_2)^{2/3}}{(R_1)^{2/3}} = \frac{(13.5)^{2/3}}{(41.9)^{2/3}} = 0.47$$

$$V_{2_{AVG}} = 0.47\ (V_{1_{AVG}}) = 0.47\ (0.85\ V_{MEAS})$$

$\boxed{V_{2_{AVG}} = 0.40\ V_{MEAS}}$ AVERAGE VELOCITY THRU SEC 2

Figure 3. Example of computation of V_{avg} from NOS current velocity data at Pensacola Bay entrance

PART III: ANALYTICAL PROCEDURE

13. The data contained in Table 1 were grouped into three main categories, namely: (1) all inlets, (2) unjettied or single-jettied inlets, and (3) inlets with two jetties. Single-jettied inlets were not analyzed separately due to the paucity of data available for these inlets. Within each of these three main categories, the data were further subdivided into: (a) inlets on all three coasts, (b) inlets on the Atlantic coast, (c) inlets on the Gulf coast, and (d) inlets on the Pacific coast. For 11 of the 12 data groupings, the one exception being the Gulf coast inlets with two jetties, sufficient data were available to warrant a regression analysis to determine the equations that best fit the data. As a first step in the analysis, the form of the best-fit equation for each set of data was determined by fitting six different functions, ranging from linear to hyperbolic, to the data. As a result of this initial analysis, a power function of the form

$$A = CP^n \tag{18}$$

where C and n are constants determined by the regression analysis, provided the best fit for all 11 data sets. The linear transform of Equation 18 is

$$\ln A = \ln C + n \ln P \tag{19}$$

14. Having established the form of the best-fit equation for the 11 sets of data, a more detailed regression analysis was performed on each set of data and 95 percent confidence limits were established for the regression constants C and n as well as for the linear form of the equations. A summary of the least-squares regression equations determined for each data set is contained in Table 2 along with the 95 percent confidence limit of the cross-sectional area (A) for the mean value of the tidal prism (P) for each set of data. In this last instance, the confidence limits are for the linear form of the equations, i.e., in

natural logarithms. Graphical representations of each of these 11 curves are shown in Plates 1-11, along with a plot of the 95 percent confidence limits and each data point used to determine the regression equation. Superposition plots of the various curves related to all inlets, inlets with one or no jetties, and inlets with two jetties are shown in Plates 12, 13, and 14, respectively.

PART IV: DISCUSSION OF RESULTS

15. From the superposition plots given in Plates 12-14, and the information contained in Table 2, the following observations can be made:

- a. For the same tidal prism, unjettied or single-jettied inlets on the Atlantic coast appear to have larger cross-sectional areas than unjettied or single-jettied inlets on the Pacific coast (Plate 13).
- b. Equations for unjettied or single-jettied inlets on the Atlantic and Pacific coasts have larger exponents (n) than do equations for inlets with two jetties on these coasts.
- c. The P versus A equation for the unjettied Gulf coast inlets closely approximates the equation computed for all inlets with two jetties (compare Equation 2c with Equation 3a in Table 2).
- d. There appears to be a slight difference in the P versus A relationship for inlets with two jetties on the Atlantic and Pacific coasts.

16. The differences between the curves for unjettied or single-jettied inlets on the Atlantic and Pacific coasts as indicated in 13a above could be caused by the differences in the computational methods used to determine the tidal prisms or they could be related to the differences in wave and/or tide characteristics that exist between these two coasts.

17. The majority of the tidal prisms computed by O'Brien[2,3] and Johnson[6] for the Pacific coast inlets, which constitute the major source of data used to compute the regression equations for this coast, were determined by multiplying the surface area of the bay by a tide range at or near the entrance to the bay. Inasmuch as this particular method does not account for phase and tide range differences that may exist for various locations within the bay, the resulting tidal prisms may be large compared with the tidal prisms computed by the cubature method. On the other hand, the data points computed by the cubature and NOS current methods for the Atlantic coast inlets generally plot below the other data points for this coast; therefore, the elimination of these points from the regression analysis would result in an equation that would predict slightly larger cross-sectional areas for a given tidal

prism. The cumulative effect of both of these factors would be to draw the two equations into closer agreement.

18. In order to determine the influence that the tidal prisms computed by the cubature and NOS current methods have on the regression equation for unjettied or single-jettied inlets on the Atlantic coast, computations were made excluding these data points. The resulting equation was:

$$A = 5.44 \times 10^{-6} P^{1.06} \tag{20}$$

which predicts smaller cross-sectional areas than the equation using all of the data (Equation 2b in Table 2), but still predicts larger areas than the comparable regression equation for the Pacific coast. Comparison of Equation 20, which was computed using 16 data points, with Equation 2b in Table 2, which was computed using 50 data points, through covariance analysis indicated that statistically no significant difference exists between the regression constants C and n. Therefore, an additional covariance analysis was performed between Equations 2b and 2d in Table 2, i.e., the equations for the unjettied and single-jettied inlets on the Atlantic and Pacific coasts, respectively, to determine whether or not the differences between these two equations are statistically significant. From the results of this covariance analysis and consideration of the 95 percent confidence limits shown in Table 2, the following can be concluded:

a. The n exponents of these two regression equations are greater than unity and could possibly be equal, i.e., the curves could be parallel.

b. There is a high degree of confidence that the C coefficients for these two equations are unequal, with the coefficient for the Atlantic coast equation being greater than that for the Pacific coast.

c. In light of a and b above, there is a high degree of confidence that unjettied or single-jettied inlets on the Atlantic coast do have larger cross sections for a given tidal prism than do their counterparts on the Pacific coast.

A discussion of the possible reasons for these differences follows.

19. Consideration must first be given to some of the sources of error that are inherent in the computational procedures for both the cubature and NOS current data methods. Error is introduced in the cubature method by using bay areas that are means of the high- and low-water areas. For bays with large expanses of marshlands which are inundated during only part of the tidal cycle, considerable variation will exist between high- and low-water areas which the mean areas may not adequately describe. Also, since bay areas were measured from NOS navigation charts which are not frequently updated except in the vicinity of navigation channels, the bay areas used in the computation may not represent the bay areas existing at the time the minimum cross-sectional areas were measured and for which the average tide curves were developed. With the NOS current method, error is introduced by the inability to obtain changes in the flow cross-sectional areas due to channel beds adjusting themselves to changes in velocity over the tidal cycle. In addition, it was assumed that such variables as sediment size, range of ocean tides, bay planform geometry and depth, freshwater input, and wave climate would not affect the computations. Although it is assumed that any errors introduced by these procedures and assumptions are small in magnitude, they may account for some of the differences observed between the various regression analyses.

20. The characteristics of the astronomical tides differ markedly between the Atlantic and Pacific coasts. However, these differences appear to be of minor importance with respect to their influence on the P versus A relationships for unjettied and single-jettied inlets. Tides on the Atlantic coast are semidiurnal, i.e., two highs and two lows of almost equal magnitude occur each day, whereas on the Pacific coast tides have a distinct diurnal inequality, i.e., there is a relatively large difference in heights of successive high and low waters. Although there is a difference in the shapes of the tide curves, the magnitudes of the tidal ranges do not differ appreciably between the two coasts. For example, the maximum ocean tide range recorded in the NOS Tide Tables for the Pacific coast occurs in the vicinity of Willapa Bay and Grays Harbor, Washington, which have a mean range of 6.5 ft and a

diurnal range of 8.6 ft. Excluding the northern coast of New England (since no tidal prism area data for this region were used in the computation of the regression equations), the maximum ocean tides on the Atlantic side occur along the Georgia coast where the mean range is about 6.8 ft and the spring range is 8.0 ft.

21. The tides are important insofar as they are responsible for generating currents in the inlets. In this respect, the NOS Tidal Current Tables[9] contain information on the annual average maximum velocities for several of the inlets used in this study. Averages of these velocities for inlets on the Atlantic, Gulf, and Pacific coasts were computed and are summarized in Table 3. Although current velocity data are given for only 4 unjettied and single-jettied inlets on the Pacific coast, the average flood and ebb velocities for these 4 inlets are almost equal to the average velocities computed for the 21 unjettied and single-jettied inlets on the Atlantic coast. Since tidal currents are the primary movers of sediment in inlets, it would appear that unjettied and single-jettied inlets on both the Atlantic and Pacific coasts are equal with regard to accommodating transportation of sediment.

22. A possible explanation for the observed differences in the P versus A relationship for these inlets could be attributable to wave climates. C. J. Galvin et al.[10] have compiled information on the mean wave conditions along the Atlantic, Gulf, and Pacific coasts. The results of Galvin's compilation are shown in Figures 4 and 5 for mean monthly wave heights and periods, respectively, and indicate that mean wave heights and periods on the Pacific coast are considerably larger than those on the Atlantic coast. Inasmuch as wave energy is a function of the square of the wave height and since littoral transport is a function of wave energy, the amount of littoral sediment entering the Pacific coast inlets should be considerably greater than that entering the Atlantic coast inlets. For a given amount of tidal energy (tidal energy being a function of the tidal currents), an inlet would be capable of accommodating a certain volume of sediment transport. Since a greater volume of sediment is apparently deposited in the Pacific coast inlets from the littoral regime, a relatively smaller portion of the

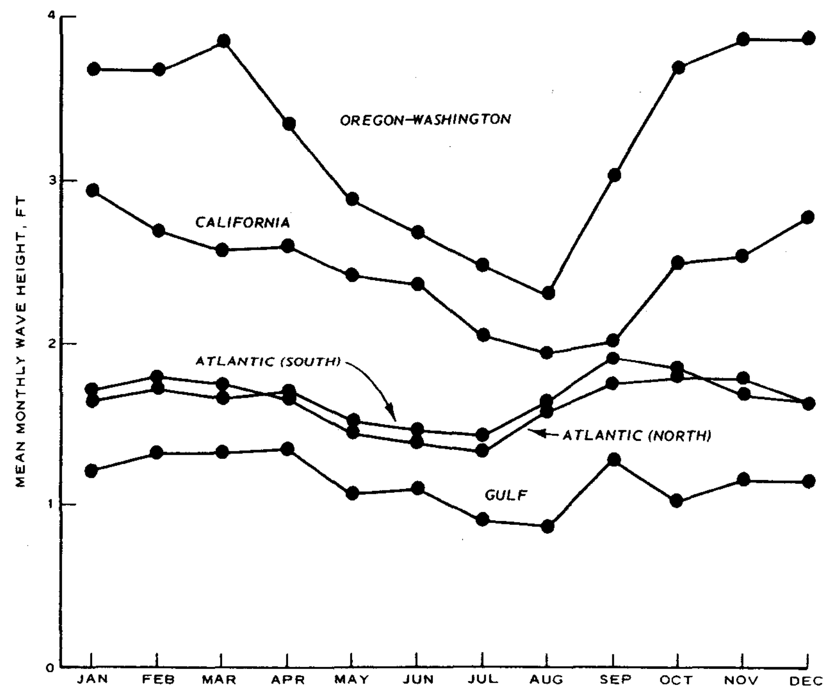

Figure 4. Mean monthly wave heights for five coastal segments[10]

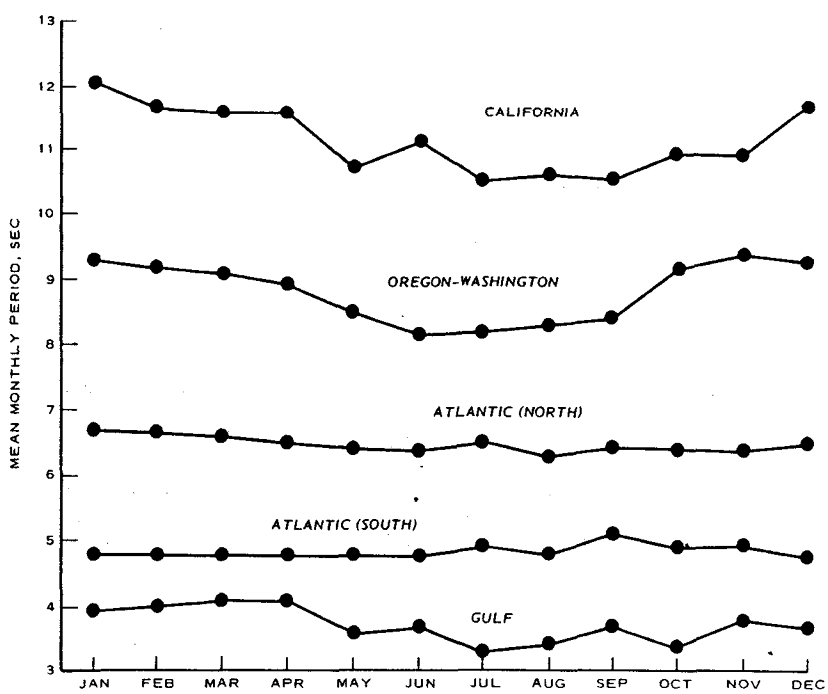

Figure 5. Mean monthly wave periods (including calms) for five coastal segments[10]

total tidal energy would be available to scour and enlarge the inlet compared with the Atlantic coast inlets.

23. Another indication that unjettied or single-jettied Pacific coast inlets have smaller cross sections than those of the Atlantic coast inlets is given by the ratio of the width of the inlet at mean sea level (W) to its hydraulic radius at mean sea level (R). This ratio is given for several inlets in Table 1, and a summary of the distribution of the W/R ratios for inlets on the Atlantic, Gulf, and Pacific coasts is given in Table 4. Although data are available for only six unjettied and single-jettied inlets on the Pacific coast, the average value of W/R for these inlets does appear to be significantly smaller than that for similar type inlets on the Atlantic coast, especially since only one of these inlets has a W/R ratio larger than 200 (Willapa Bay with W/R = 1303). The significance of a small value of W/R is that the channel is narrow and deep and consequently should be hydraulically more efficient than a wide and shallow channel. Therefore, unjettied or single-jettied inlets on the Pacific coast can accommodate larger volumes of water per unit area than inlets on the Atlantic coast. The reason for the small values of W/R for the Pacific coast inlets is not known, but it is probably related to the higher rates of littoral drift that enters the inlets.

24. Regression equations computed for inlets with two jetties compared with unjettied and single-jettied inlets essentially agree with the findings of O'Brien, Johnson, and Nayak, i.e., the exponents (n) for unjettied and single-jettied inlets are larger than those for inlets with two jetties. In the case of O'Brien, Johnson, and Nayak, their exponents were unity for unjettied inlets, whereas the regression analysis computed exponents slightly larger than unity for unjettied and single-jettied inlets on the Atlantic and Pacific coasts. The larger exponents for uncontrolled and semicontrolled inlets indicate that a unit change in the tidal prism through these inlets will result in larger changes in the cross-sectional area than those which would occur in a controlled inlet for a similar change in the tidal prism. This is due to the lateral restrictions jetties impose on an inlet, resulting in these inlets

developing narrow and deep channels that are hydraulically more efficient than the wide and shallow channels that characterize uncontrolled or semicontrolled inlets. An indication of the relative difference in the cross-sectional configuration of jettied and unjettied or single-jettied inlets is given in Table 4 by the distribution and average values of the ratio W/R. For the most part, W/R is small for inlets with two jetties (i.e., W/R < 100) and large for unjettied and single-jettied inlets.

25. The data used to compute the regression equation for the unjettied Gulf coast inlets exhibited more scatter than the data used for the other two coasts; therefore, the prediction equation for P versus A on the Gulf coast would appear to be less reliable. In any event, the relationship computed for the unjettied Gulf coast inlets is interesting in that it agrees closely with the regression equation computed for all inlets with two jetties.

26. Part of the scatter of the Gulf coast data may be attributed to tidal characteristics. In the Gulf of Mexico, the tides are uniformly small and vary from diurnal to semidiurnal, depending upon the declination of the moon. When the moon is near its extreme north or south declination, the tides are diurnal. As the moon nears the equator, tides in the eastern Gulf become negligible and vary only a few tenths of a foot from high water to low water. In the western Gulf, tides are small and become semidiurnal as the moon approaches the equator, although there are periods during this time in which distinct inequalities between successive highs and lows exist, much like the Pacific coast tides. As a result of these tidal variations, astronomical tidal currents through the Gulf coast inlets are sometimes weak and variable. In the NOS Tidal Current Tables, average maximum current velocities are given for 16 unjettied Gulf coast inlets used in this analysis. The average maximum velocities in these inlets (see Table 3) are 2.63 fps on flood and 2.45 fps on ebb, which are approximately 1 fps less than the average maximum velocities in the Atlantic and Pacific coast inlets.

27. Inasmuch as the Gulf coast inlets are subject to frequent periods in which the astronomical tidal currents are weak or nonexistent,

these inlets are susceptible to moderate variations in meteorological conditions. Also, since an inlet's astronomical tidal prism varies from near zero to its diurnal value, the instantaneous cross-sectional area of a Gulf coast inlet is highly dependent upon antecedent astronomical and/or meteorological tide conditions. In all instances, the cross-sectional areas of the Gulf inlets measured from NOS hydrographic surveys were related to the diurnal tidal prism. However, an NOS survey could reflect conditions at an inlet when the tidal prism had been larger than the diurnal prism due to meteorological conditions or smaller due to astronomical and/or meteorological effects. Since there are wide variations in the Gulf tidal characteristics, the relatively large scatter of the tidal prism - inlet area data cannot be due entirely to measurement error.

28. If the relationship between P and A for the Gulf coast inlets can be accepted as reasonably accurate, then the agreement between this relationship and that for all inlets with two jetties appears to be related to the wave conditions in the Gulf. Referring to Figures 4 and 5, the waves in the Gulf are relatively small, in terms of both height and period, compared with the other two coasts. Since waves appear to have a relatively minor influence on the Gulf coast inlets, the results of Nayak's model study could possibly be extrapolated to the prototype. Nayak observed that when his unjettied model inlet was operated without waves, the equilibrium cross-sectional area that developed agreed closely with that which would be predicted by the equation for jettied inlets.

29. The regression equation computed for all inlets with two jetties (Equation 3a in Table 2) predicts a cross-sectional area that is only 5.5 percent smaller than that predicted by O'Brien's equation for jettied inlets (Equation 3) for a tidal prism of 10^7 cu ft and 3.3 percent larger for a tidal prism of 10^{11} cu ft. The agreement between these two equations is quite remarkable when one considers that O'Brien[3] used only 17 data points for 17 inlets with two jetties (13 of the inlets are located on the Pacific coast) whereas Equation 3a in Table 2 was computed using 66 data points for 37 inlets (only 15 of which are

located on the Pacific coast). Even though there is good agreement between this regression equation and O'Brien's relationship, when the Atlantic and Pacific coast inlets with two jetties are considered separately, the resulting regression equations differ somewhat.

30. With respect to the Pacific coast inlets with two jetties, the exponent (n) computed by the regression analysis (see Equation 3d in Table 2) is exactly the same as that derived by O'Brien, i.e., 0.85. However, the constant (C) is about 12.6 percent larger than O'Brien's. Therefore, Equation 3d in Table 2 predicts cross-sectional areas 12.6 percent larger than O'Brien's equation. The equation for the jettied Atlantic coast inlets (Equation 3b in Table 2) varies considerably from O'Brien's. For example, with tidal prisms of 10^7 and 10^{11} cu ft, this equation predicts cross-sectional areas that are 38.1 percent smaller and 54.9 percent larger, respectively, than those predicted by Equation 3.

31. In order to determine whether or not the regression equations for jettied Atlantic and Pacific coast inlets differ significantly, a covariance analysis was performed between these two equations to test the hypothesis that the two equations are identical. Results of this analysis indicated that this hypothesis would not be rejected at the 60 percent confidence level, i.e., with the probability of making a mistake concerning this hypothesis at 40 percent, the hypothesis still holds. Statistically, this probability is too large to reject the hypothesis that the two equations are equal. Therefore, until more accurate data are available to analyze P versus A relationships for jettied inlets, O'Brien's equation (Equation 3) or Equation 3a in Table 2 should be used to estimate the cross-sectional area that an inlet should develop once jetties are installed.

32. As a further note on the design of a dual jetty system, the spacing of the jetties should be such as to yield a W/R ratio of less than 100, inasmuch as over 80 percent of the two-jettied inlets used in this analysis had ratios of W/R less than 100 (Table 4).

PART V: CONCLUSIONS

33. An attempt was made to determine whether or not differences exist between the tidal prism - inlet area relationships for inlets on the Atlantic, Gulf, and Pacific coasts of the United States. The conclusions reached from this analysis are: (a) unjettied and single-jettied inlets on the three coasts do exhibit different P versus A relationships as a result of the differences in the tidal and wave characteristics between these three coasts, and (b) the available data do not warrant any modification in the P versus A relationship for jettied inlets as originally determined by O'Brien.

REFERENCES

1. LeConte, L. J., Discussion of "Notes on the Improvement of River and Harbor Outlets in the United States," Paper No. 1009 by D. A. Watts, Transactions, American Society of Civil Engineers, Vol LV, Dec 1905, pp 306-308.

2. O'Brien, M. P., "Estuary Tidal Prisms Related to Entrance Areas," Civil Engineering, Vol 1, No. 8, 1931, pp 738-739.

3. ___________, "Equilibrium Flow Areas of Inlets on Sandy Coast," Journal, Waterways and Harbors Division, American Society of Civil Engineers, Vol 95, No. WW1, Feb 1969, pp 43-52.

4. Nayak, I. V., "Tidal Prism-Area Relationship in a Model Inlet," Technical Report HEL 24-1, Feb 1971, Hydraulic Engineering Laboratory, University of California at Berkeley, Berkeley, Calif.

5. Lin, P. M., Modeling of the Sediment Transport in the Vicinity of Inlet and Coastal Region, M.S. Thesis, University of Florida, Gainesville, Fla., 1969.

6. Johnson, J. W., "Tidal Inlets on the California, Oregon, and Washington Coasts," Technical Report HEL 24-12, 1972, Hydraulic Engineering Laboratory, University of California at Berkeley, Berkeley, Calif.

7. Delmonte, R. C. and Johnson, J. W., "The Influence of Bed Material Size on the Tidal Prism-Area Relationship in a Tidal Inlet," Technical Report HEL 24-8, Aug 1971, Hydraulic Engineering Laboratory, University of California at Berkeley, Berkeley, Calif.

8. National Ocean Survey, National Oceanic and Atmospheric Administration, "Tide Tables, East Coast North and South America, Including Greenland," and "Tide Tables, West Coast North and South America, Including the Hawaiian Islands."

9. ___________, "Tidal Current Tables, Atlantic Coast of North America," and "Tidal Current Tables, Pacific Coast of North America and Asia."

10. Galvin, C. J. et al., "Nearshore Visual Wave Observations for United States' Coastlines," 1969, U. S. Army Coastal Engineering Research Center, Washington, D. C.

11. Charlesworth, L. J., Jr., Bay, Inlet and Nearshore Marine Sedimentation: Beach Haven-Little Egg Inlet Region, New Jersey, Ph. D. Dissertation, University of Michigan, Ann Arbor, Mich., 1968.

12. U. S. Army Engineer Waterways Experiment Station, CE, "Model Study of Plans for Elimination of Shoaling in Absecon Inlet, New Jersey," Technical Memorandum No. 204-1, Sep 1943, Vicksburg, Miss.

13. Keulegan, G. H. and Hall, J. V., Jr., "A Formula for the Calculation of the Tidal Discharge Through an Inlet," Bulletin of the Beach Erosion Board, Vol 4, No. 1, Jan 1950, pp 15-29.

14. Bruun, P. and Gerritsen, F., Stability of Coastal Inlets, North Holland Publishing Co., Amsterdam, 1960.

15. Bruun, P., Gerritsen, F., and Morgan, W. H., "Florida Coastal Problems," Proceedings, Sixth Conference on Coastal Engineering, The Engineering Foundation Council on Wave Research, 1958, p 463.

16. U. S. Army Engineer District, Jacksonville, CE, "General and Detailed Design Memorandum - Ponce de Leon Inlet, Florida" (unpublished), 1967, Jacksonville, Fla.

17. Reynolds, K. C., "Report on Tidal Entrances to Beach Erosion Board, Corps of Engineers" (unpublished), 1951, Washington, D. C.

18. Keulegan, G. H., "Tidal Flow in Entrances: Water-Level Fluctuations of Basins in Communication with Seas," Technical Bulletin No. 14, Jul 1967, U. S. Army Committee on Tidal Hydraulics, CE.

19. Goodwin, C. R. et al., "Tidal Study of Three Oregon Estuaries," Bulletin No. 45, 1970, Engineering Experiment Station, Oregon State University, Corvallis, Oreg.

20. Committee on Tidal Hydraulics, CE, "Tillamook Bay, Oregon," Jan 1970, U. S. Army Engineer Waterways Experiment Station, CE, Vicksburg, Miss.

Table 1

Tidal Prism and Cross-Sectional Area Data

Inlet/Data Source	Spring or Diurnal Tidal Prism, P cu ft	MSL Area A sq ft	Hydraulic Radius R ft	W/R Ratio	Maximum Currents from NOS Tidal Current Tables fps Flood	Ebb
		Atlantic Coast Inlets Without Jetties				
1. Plum Island Sound, Mass.					2.70	2.53
NOS Current Data, Oct 1953	1.32×10^9	3.98×10^4	17.6	128		
2. Fire Island Inlet, N. Y.					4.05	4.05
a. O'Brien (3)	2.18×10^9	3.56×10^4				
b. Cubature (NOS 1933)	1.86×10^9	4.01×10^4	14.7	195		
3. Jones Inlet, N. Y.					5.24	4.39
a. O'Brien (3)	1.50×10^9	2.89×10^4				
b. Cubature (NOS 1933)	1.04×10^9	2.04×10^4	15.4	86		
c. NOS Current Data, Jul 1933	1.02×10^9	2.04×10^4	15.4	86		
4. Beach Haven Inlet (Little Egg Bay), N. J.						
Cubature (NOS 1936)	1.51×10^9	2.53×10^4	9.3	293		
5. Little Egg Inlet (Great Bay), N. J.						
a. Cubature (NOS 1935)	1.72×10^9	3.83×10^4	13.3	216		
b. L. J. Charlesworth (11)	(1.93×10^9)					
6. Brigantine Inlet, N. J.						
Cubature (NOS 1936)	5.23×10^8	1.22×10^4	19.2	33		
7. Absecon Inlet (before jetties), N. J.						
WES Model Report (12)	1.65×10^9	2.66×10^4	35.6	21		
8. Great Egg Harbor Entr, N. J.						
Cubature (NOS 1936-37)	2.00×10^9	7.01×10^4	12.3	460		
9. Townsend Inlet, N. J.						
Cubature (NOS 1937)	5.56×10^8	1.42×10^4	18.8	40		
10. Hereford Inlet, N. J.						
Cubature (NOS 1937)	1.19×10^9	3.57×10^4	12.0	246		
11. Chincoteague Inlet, Va.						
Cubature (NOS 1934)	1.56×10^9	4.44×10^4	7.9	712		
12. Oregon Inlet, N. C.						
Corps of Engrs, 1965 Flow Meas	3.98×10^9	6.66×10^4	13.5	367		
13. Ocracoke Inlet, N. C.					2.87	4.05
Corps of Engrs, 1950 Flow Meas	5.22×10^9	9.68×10^4	13.8	435		
14. Drum Inlet, N. C.						
Corps of Engrs, 1936 Flow Meas	5.82×10^8	7.70×10^3				
15. Beaufort Inlet, N. C.					2.53	2.53
a. Corps of Engrs, 1935-36 Flow Meas	5.0×10^9	8.66×10^4	17.5	250		
b. Keulegan-Hall (13)	(5.1×10^9)					
16. Carolina Beach Inlet, N. C.						
Corps of Engrs, 1967 Flow Meas	5.25×10^8	7.6×10^3	13.2	44		
17. Stono Inlet, S. C.					3.21	4.56
NOS Current Data, May 1934	2.86×10^9	5.43×10^4	10.3	819		
18. North Edisto River, S. C.					4.90	6.25
O'Brien (3)	4.58×10^9	9.95×10^4				
19. St. Helena Sound, S. C.						
Cubature (NOS 1934)	1.53×10^{10}	4.66×10^5	21.2	1040		
20. Port Royal Sound, S. C.					3.04	3.04
Cubature (NOS 1934)	1.46×10^{10}	5.41×10^5	42.6	298		
21. Calibogue Sound, S. C.					3.72	4.22
Cubature (NOS 1934)	3.61×10^9	1.53×10^5	38.0	106		
22. Wassaw Sound, Ga.					2.87	3.72
NOS Current Data, 1934	8.2×10^9	2.64×10^5	17.9	824		
23. Ossabaw Sound, Ga.					2.70	3.21
Cubature (NOS 1934)	6.81×10^9	3.17×10^5	16.4	1180		
24. Sapelo Sound, Ga.					3.55	4.22
a. Cubature (NOS 1934)	7.36×10^9	2.16×10^5	24.9	348		
b. NOS Current Data, 1934	6.12×10^9	2.16×10^5	24.9	348		

(Continued)

Note: Data in parentheses not used in analyses.

Table 1 (Continued)

Inlet/Data Source	Spring or Diurnal Tidal Prism, P cu ft	MSL Area A sq ft	Hydraulic Radius R ft	W/R Ratio	Maximum Currents from NOS Tidal Current Tables fps Flood	Ebb
Atlantic Coast Inlets Without Jetties (Continued)						
25. St. Catherines Sound, Ga.					3.21	3.55
a. Cubature (NOS 1934)	6.94×10^9	2.39×10^5	31.2	246		
b. NOS Current Data, 1934	8.3×10^9	2.39×10^5	31.2	246		
26. Doboy Sound, Ga.					3.38	3.38
Cubature (NOS 1934)	4.04×10^9	9.91×10^4	23.7	177		
27. Altamaha Sound, Ga.					1.69	3.21
Cubature (NOS 1934)	2.91×10^9	9.23×10^4	8.4	1310		
28. Hampton River, Ga.						
Cubature (NOS 1934)	1.01×10^9	4.11×10^4	22.7	80		
29. St. Simon Sound, Ga.					3.55	3.21
a. Cubature (NOS 1934)	6.54×10^9	2.51×10^5	34.2	180		
b. NOS Current Data, Mar 1934	1.35×10^{10}	2.51×10^5	34.2	180		
30. St. Andrew Sound, Ga.					3.55	3.72
a. Cubature (NOS 1934-35)	9.86×10^9	3.85×10^5	27.0	528		
b. NOS Current Data 1934	7.0×10^9	2.31×10^5				
31. Nassau Sound, Fla.					2.87	2.87
Cubature (NOS 1934)	2.20×10^9	7.25×10^4	15.0	322		
32. Ft. George Inlet, Fla.						
Cubature (NOS 1954)	3.11×10^8	8.6×10^3	6.0	239		
33. Old St. Augustine Inlet, Fla.						
Bruun and Gerritsen (14)	1.31×10^9	2.65×10^4				
34. Ponce de Leon, Fla. (before jetties)						
a. Cubature	5.74×10^8					
b. Corps of Engrs, G.D.M. (16)	6.19×10^8					
c. Bruun and Gerritsen (14)	5.65×10^8	1.15×10^4	12.8	70		
35. Delaware Bay Entrance					3.04	3.21
O'Brien (3)	1.25×10^{11}	2.5×10^6				
Atlantic Coast Inlets with One Jetty						
36. Fire Island Inlet, N. Y.						
Corps of Engrs, Aug 1965 Flow Meas	1.86×10^9	3.81×10^4	11.7	278		
37. East Rockaway Inlet, N. Y.					3.72	3.88
a. O'Brien (3)	7.6×10^8	1.15×10^4				
b. Cubature (NOS 1934)	4.86×10^8	1.18×10^4	16.6	43		
c. NOS Current Data, 1934	4.0×10^8	1.18×10^4	16.6	43		
38. Rockaway Inlet, N. Y.					3.04	4.56
a. O'Brien (3)	3.7×10^9	8.6×10^4				
b. NOS Current Data, Sep 1934	3.4×10^9	1.23×10^5	23.0	233		
39. Masonboro Inlet, N. C.						
Corps of Engrs, Sep 1969 Flow Meas	8.55×10^8	1.27×10^4	12.7	79		
40. St. Lucie Inlet, Fla.						
a. Cubature (NOS 1930)	5.94×10^8	1.76×10^4	9.2	208		
b. Corps of Engrs, Jacksonville Dist	5.66×10^8					
Atlantic Coast Inlets with Two Jetties						
41. Nantucket Inlet, Mass.					2.03	2.53
Keulegan-Hall (13)	4.32×10^8	1.26×10^4	12.8	77		
42. Shinnecock Inlet, N. Y.					4.22	3.88
Cubature (CE Area)	2.19×10^8	5.5×10^3				
43. Moriches Inlet, N. Y.						
a. O'Brien (3)	1.57×10^9	2.04×10^4				
b. Corps of Engrs, 1967-68 Flow Meas	8.46×10^8	1.32×10^4	14.4	64		
44. Shark River Inlet, N. J.						
Cubature	1.48×10^8	3.00×10^3	13.2	17		

(Continued)

Table 1 (Continued)

Inlet/Data Source	Spring or Diurnal Tidal Prism, P cu ft	MSL Area A sq ft	Hydraulic Radius R ft	W/R Ratio	Maximum Currents from NOS Tidal Current Tables fps Flood	Ebb
Atlantic Coast Inlets with Two Jetties (Continued)						
45. Manasguan Inlet, N. J.					2.87	3.04
a. Cubature (NOS 1934)	1.75×10^8	5.19×10^3	12.3	34		
b. Keulegan-Hall (13)	1.745×10^8					
46. Barnegat Inlet, N. J.					3.52	4.22
a. Cubature (NOS 1936)	6.25×10^8	1.48×10^4	14.2	73		
b. Corps of Engrs, 1940-41 Flow Meas	1.18×10^9	1.62×10^4				
c. Corps of Engrs, 1943 Flow Meas	7.5×10^8	1.09×10^4				
d. Corps of Engrs, 1945 Flow Meas	7.1×10^8	1.34×10^4				
e. Corps of Engrs, 1968 Flow Meas	6.25×10^8	9.25×10^3				
47. Absecon Inlet, N. J.						
O'Brien (3)	1.48×10^9	3.13×10^4				
48. Cold Springs Harbor (Cape May), N. J.					3.04	3.72
a. NOS Current Data, 1947	6.50×10^8	1.29×10^4	17.1	44		
b. Bruun, Gerritsen, and Morgan (15)	1.70×10^8	4.60×10^3				
c. Reynolds (17)	3.35×10^8	1.16×10^4	15.2	50		
49. Indian River Inlet, Del.					3.04	3.55
Keulegan (18)	5.25×10^8	9.66×10^3	12.0	67		
50. Winyah Bay, S. C.					3.21	3.38
Cubature (NOS 1935)	3.02×10^9	7.86×10^4	19.7	203		
51. Charleston, S. C.					3.04	3.04
O'Brien (3)	5.75×10^9	1.44×10^5				
52. Savannah River (Tybee Roads), Ga.					2.7	4.39
NOS Current Data, Apr-May 1934	3.1×10^9	5.87×10^4	24.2	100		
53. St. Marys (Fernandina Harbor), Fla.					3.88	4.39
a. Cubature (NOS 1937)	4.77×10^9	1.44×10^5	33.2	130		
b. Bruun, Gerritsen, and Morgan (15)	6.20×10^9	1.50×10^5				
54. St. Johns River, Fla.					3.21	3.88
a. Cubature (NOS 1958-59)	1.73×10^9	5.73×10^4	38.5	39		
b. Bruun, Gerritsen, and Morgan (15)	1.90×10^9	3.60×10^4				
c. Corps of Engrs, Jacksonville Dist	3.92×10^9					
55. Fort Pierce Inlet, Fla.					4.39	5.24
NOS Current Data, May 1930	5.81×10^8	1.20×10^4	13.6	65		
56. Jupiter Inlet, Fla.						
a. Cubature (NOS 1967)	1.11×10^8	2.91×10^3	9.0	36		
b. Corps of Engrs, Jacksonville Dist	1.02×10^8					
57. Lake Worth Inlet, Fla.					4.05	6.08
a. NOS Current Data, Apr 1929	9.0×10^8	9.5×10^3	13.2	73		
b. Bruun, Gerritsen, and Morgan (15)	8.3×10^8	1.52×10^4				
c. Corps of Engrs, Jacksonville Dist	9.32×10^8					
58. Port Everglades, Fla.					1.01	1.18
NOS Current Data, Feb 1967	3.0×10^8	2.1×10^4	30.4	23		
59. Bakers Haulover, Fla.					4.90	4.22
Keulegan and Hall (13)	3.6×10^8	4.38×10^3	11.9	31		
Gulf Coast Inlets Without Jetties						
60. Captiva Pass, Fla.					3.04	3.21
NOS Current Data, Aug 1960	1.90×10^9	2.87×10^4	15.2	125		
61. Boca Grande Pass, Fla.					3.72	3.04
NOS Current Data, 1959	1.26×10^{10}	1.66×10^5	31.8	164		
62. Gasparilla Pass, Fla.					1.69	1.86
a. NOS Current Data, Nov 1958	4.7×10^8	1.33×10^4	8.5	185		
b. Bruun and Gerritsen (14)	4.0×10^8	1.05×10^4				
63. Stump Pass, Fla.						
Cubature (NOS 1955-56)	3.61×10^8	5.90×10^3	7.9	94		

Table 1 (Continued)

Inlet/Data Source	Spring or Diurnal Tidal Prism, P cu ft	MSL Area A sq ft	Hydraulic Radius R ft	W/R Ratio	Maximum Currents from NOS Tidal Current Tables fps Flood	Ebb
Gulf Coast Inlets Without Jetties (Continued)						
64. Midnight Pass, Fla.					3.04	2.36
a. Cubature (NOS 1955)	2.61×10^8	3.22×10^3	7.0	66		
b. NOS Current Data, Mar 1955	2.84×10^8	3.22×10^3	7.0	66		
65. Big Sarasota Pass, Fla.					2.53	1.69
NOS Current Data, Mar-Apr 1955	7.6×10^8	2.31×10^4	12.3	153		
66. New Pass, Fla.					2.70	1.69
NOS Current Data, Sep 1953	4.00×10^8	6.37×10^3	11.4	49		
67. Longboat Pass, Fla.					3.04	2.70
a. NOS Current Data, Oct 1953	4.90×10^8	1.14×10^4	14.5	54		
b. Bruun and Gerritsen (14)	7.77×10^8	1.13×10^4		59		
68. Sarasota Pass, Fla.						
Cubature	8.10×10^8	1.99×10^4	4.2	1132		
69. Pass-a-Grille					2.03	2.36
NOS Current Data, Apr 1950	1.42×10^9	3.5×10^4	17.7	112		
70. Johns Pass, Fla.					3.38	2.53
a. Cubature (NOS 1951-52)	5.03×10^8	8.86×10^3	14.9	40		
b. NOS Current Data, May 1949	4.96×10^8	8.42×10^3	13.3	47		
71. Little (Clearwater) Pass, Fla.					2.20	1.86
a. NOS Current Data, Jun 1951	6.8×10^8	2.23×10^4	6.3	560		
b. Bruun, Gerritsen, and Morgan (15)	5.2×10^8	1.70×10^4				
72. Big (Dunedin) Pass, Fla.					1.69	1.69
a. NOS Current Data, Jun 1959	3.76×10^8	1.44×10^4	7.8	237		
b. Bruun and Gerritsen (14)	3.18×10^8	6.0×10^3		191		
73. East (Destin) Pass, Fla.						
a. Bruun and Gerritsen (14)	1.62×10^9	1.38×10^4		191		
b. Corps of Engrs, 1938 Flow Meas	1.57×10^9	1.72×10^4	11.1	141		
74. Pensacola Bay Entr., Fla.					2.70	3.04
a. NOS Current Data, Apr 1940	9.45×10^9	1.12×10^5	32.7	105		
b. Bruun, Gerritsen, and Morgan (15)	6.80×10^9	1.20×10^5				
75. Perdido Pass, Ala.						
Corps of Engrs, 1963 Flow Meas	5.84×10^8	7.00×10^3				
76. Mobile Bay Entr., Ala.					2.36	2.53
a. NOS Current Data, Jun 1935	2.0×10^{10}	3.15×10^5	18.3	940		
b. Corps of Engrs, 1972 Flow Meas	3.4×10^{10}	3.14×10^5				
77. Barataria Pass, La.					2.53	2.20
NOS Current Data, 1947	2.55×10^9	6.93×10^4	31.7	69		
78. Caminada Pass, La.					2.53	2.53
NOS Current Data, 1933-34	6.34×10^8	1.26×10^4	7.4	232		
79. Calcasieu Pass, La.					2.87	3.88
Bruun and Gerritsen (14)	2.97×10^9	2.08×10^4		29		
80. San Luis Pass, Tex.						
Cubature (NOS 1933-34)	5.84×10^8	3.20×10^4	7.4	584		
Gulf Coast Inlets with Two Jetties						
81. Venice Inlet, Fla.					1.86	1.52
a. Cubature (NOS 1955)	8.5×10^7	2.36×10^3	9.1	29		
b. NOS Current Data, May 1955	7.4×10^7	2.36×10^3	9.1	29		
c. Corps of Engrs, Jacksonville Dist	9.41×10^7					
82. Galveston Entr., Tex.					2.87	3.88
a. O'Brien (3) including San Luis Pass	1.59×10^{10}	2.2×10^5				
b. Cubature (NOS 1934)	5.94×10^9	1.97×10^5				
83. Aransas Pass, Tex.					1.52	2.03
a. Bruun and Gerritsen (14)	1.76×10^9	1.6×10^4				
b. Reynolds (17)	6.66×10^9	2.73×10^4				

(Continued)

Table 1 (Continued)

Inlet/Data Source	Spring or Diurnal Tidal Prism, P cu ft	MSL Area A sq ft	Hydraulic Radius R ft	W/R Ratio	Maximum Currents from NOS Tidal Current Tables fps Flood	Ebb
Pacific Coast Inlets Without Jetties						
84. Willapa Bay, Wash.					4.22	4.22
a. O'Brien (3)	2.50×10^{10}	3.94×10^{5}				
b. Johnson (6)	1.73×10^{10}	4.95×10^{5}	19.5	1303		
85. Siletz Bay, Oreg.						
Oregon St Univ (19)	3.5×10^{8}	3.4×10^{3}				
86. Alsea Bay, Oreg.						
Oregon St Univ (19)	5.0×10^{8}	8.0×10^{3}				
87. Tomales Bay, Calif.						
a. O'Brien (3)	1.58×10^{9}	3.6×10^{4}				
b. Johnson (6)	1.49×10^{9}	2.12×10^{4}	16.0	83		
88. Bolinas Lagoon, Calif.						
Johnson (6)	1.31×10^{8}	1.3×10^{3}	6.6	30		
89. San Francisco, Calif.					4.05	4.39
a. O'Brien (3)	5.1×10^{10}	9.38×10^{5}				
b. Johnson (6)	5.1×10^{10}	9.31×10^{5}	177	30		
90. Newport Bay, Calif. (before jetties)						
Reynolds (17)	3.77×10^{8}	3.7×10^{3}				
91. Punta Banda						
O'Brien (3)	2.99×10^{8}	5.46×10^{3}				
Pacific Coast Inlets with One Jetty						
92. Tillamook Bay, Oreg.					5.07	4.39
a. O'Brien (3)	2.11×10^{9}	3.69×10^{4}				
b. Johnson (6)	2.15×10^{9}	1.57×10^{4}	10.6	140		
c. Comm Tidal Hyd (20)	2.49×10^{9}	2.70×10^{4}				
93. San Diego Bay, Calif.					2.03	2.53
a. O'Brien (3)	3.38×10^{9}	6.17×10^{4}				
b. Johnson (6)	2.52×10^{9}	7.12×10^{4}	38.0	48		
Pacific Coast Inlets with Two Jetties						
94. Grays Harbor, Wash.					3.21	4.73
a. O'Brien (3)	2.43×10^{10}	2.85×10^{5}				
b. Johnson (6)	1.70×10^{10}	2.91×10^{5}	43	158		
c. Bruun and Gerritsen (14)	1.84×10^{10}	3.36×10^{5}				
95. Columbia River, Oreg., Wash.					6.08	7.09
a. O'Brien (3)	3.82×10^{10}	5.08×10^{5}				
b. Johnson (6)	3.87×10^{10}	4.43×10^{5}	37.5	315		
96. Nehalem River, Oreg.						
a. O'Brien (3)	6.0×10^{8}	1.12×10^{4}				
b. Johnson (6)	5.66×10^{8}	9.64×10^{3}	17.5	31		
97. Yaquina Bay, Oreg.					4.05	3.88
a. O'Brien (3)	7.73×10^{8}	1.98×10^{4}				
b. Johnson (6)	1.12×10^{9}	1.96×10^{4}	19.6	51		
c. Oregon St Univ (19)	1.12×10^{9}	2.20×10^{4}				
98. Siuslaw River, Oreg.					1.52	1.86
a. O'Brien (3)	4.64×10^{8}	1.10×10^{4}				
b. Johnson (6)	3.66×10^{8}	8.33×10^{4}	11.2	67		
c. Comm Tidal Hyd (20)	4.82×10^{8}					
99. Umpqua River, Oreg.					1.35	1.69
a. O'Brien (3)	2.20×10^{9}	4.62×10^{4}				
b. Johnson (6)	1.59×10^{9}	3.3×10^{4}	16.7	119		
c. Comm Tidal Hyd (20)	2.20×10^{9}	3.8×10^{4}				
100. Coos Bay, Oreg.					3.04	3.72
a. O'Brien (3)	2.84×10^{9}	6.11×10^{4}				
b. Johnson (6)	2.51×10^{9}	5.65×10^{4}	27.4	75		
c. Comm Tidal Hyd (20)	2.51×10^{9}	5.40×10^{4}				

(Continued)

Table 1 (Concluded)

Inlet/Data Source	Spring or Diurnal Tidal Prism, P cu ft	MSL Area A sq ft	Hydraulic Radius R ft	W/R Ratio	Maximum Currents from NOS Tidal Current Tables fps Flood	Ebb
Pacific Coast Inlets with Two Jetties (Continued)						
101. Coquille River, Oreg.					2.36	2.03
a. O'Brien (3)	3.89×10^8	9.02×10^3				
b. Johnson (6)	1.77×10^8	7.03×10^3	11.3	55		
c. Comm Tidal Hyd (20)	(3.89×10^8)					
102. Rogue River, Oreg.					2.02	2.02
Comm Tidal Hyd (20)	1.51×10^8	4.5×10^3				
103. Humboldt Bay, Calif.					2.70	3.38
a. O'Brien (3)	4.38×10^9	7.55×10^4				
b. Johnson (6)	3.51×10^9	5.19×10^4	23.6	93		
104. Bodega Bay, Calif.						
Johnson (6)	1.49×10^8	5.12×10^3	16.4	19		
105. Moss Landing, Calif.						
Johnson (6)	1.41×10^8	4.12×10^3	10.7	36		
106. Newport Bay, Calif.						
a. O'Brien (3)	1.09×10^8	5.98×10^3				
b. Reynolds (17)	3.31×10^8	1.0×10^4				
107. Camp Pendleton, Calif.						
O'Brien (3)	1.14×10^7	4.64×10^2				
108. Mission Bay, Calif.						
a. O'Brien (3)	4.2×10^8	1.04×10^4				
b. Johnson (6)	4.7×10^8	1.59×10^4	15.9	63		
c. Bruun and Gerritsen (14)	4.24×10^8	8.5×10^3		236		

Table 2

Regression Equations of P Versus A ; Form of Equations $A = CP^n$

Equation	95% Confidence Limits of C: Lower	95% Confidence Limits of C: Upper	95% Confidence Limits of n: Lower	95% Confidence Limits of n: Upper	Width of 95% Confidence Limits of A for Mean P Natural Logarithms	Number of Data Points
1. All Inlets						
a. Atlantic, Gulf, and Pacific coasts $A = 5.74 \times 10^{-5}P^{0.95}$	5.36×10^{-5}	6.13×10^{-5}	0.91	1.00	1.70615	162
b. Atlantic coast $A = 7.75 \times 10^{-6}P^{1.05}$	7.14×10^{-6}	8.41×10^{-6}	0.99	1.12	1.46894	79
c. Gulf coast $A = 5.02 \times 10^{-4}P^{0.84}$	4.25×10^{-4}	5.93×10^{-4}	0.73	0.95	2.03012	36
d. Pacific coast $A = 1.19 \times 10^{-4}P^{0.91}$	1.07×10^{-4}	1.32×10^{-4}	0.86	0.97	1.45688	47
2. Unjettied or Single-Jettied Inlets						
a. Atlantic, Gulf, and Pacific coasts $A = 1.04 \times 10^{-5}P^{1.03}$	9.47×10^{-6}	1.13×10^{-5}	0.97	1.10	1.78570	96
b. Atlantic coast $A = 5.37 \times 10^{-6}P^{1.07}$	4.86×10^{-6}	5.92×10^{-6}	0.99	1.16	1.40610	50
c. Gulf coast $A = 3.51 \times 10^{-4}P^{0.86}$	2.97×10^{-4}	4.16×10^{-4}	0.73	0.99	1.86524	30
d. Pacific coast $A = 1.91 \times 10^{-6}P^{1.10}$	1.57×10^{-6}	2.32×10^{-6}	0.99	1.21	1.61031	16
3. Inlets with Two Jetties						
a. Atlantic, Gulf, and Pacific coasts $A = 3.76 \times 10^{-4}P^{0.86}$	3.44×10^{-4}	4.11×10^{-4}	0.81	0.92	1.44345	66
b. Atlantic coast $A = 5.77 \times 10^{-5}P^{0.95}$	4.98×10^{-5}	6.69×10^{-5}	0.81	1.09	1.61274	29
c. Gulf coast Insufficient data for regression analysis						
d. Pacific coast $A = 5.28 \times 10^{-4}P^{0.85}$	4.96×10^{-4}	5.23×10^{-4}	0.81	0.88	0.71289	31

Table 3

Annual Average Maximum Velocities in Tidal Inlets from NOS Tidal Current Tables for Inlets Used to Determine P Versus A Relationships

Coast/Type of Inlet	Number of Inlets	Average Maximum Flood Velocity, fps	Average Maximum Ebb Velocity, fps
Atlantic			
Unjettied or single jetty	21	3.33	3.73
Two jetties	14	3.43	3.97
All inlets	35	3.37	3.83
Gulf			
Without jetties	16	2.63	2.45
Two jetties	3	2.08	2.48
All inlets	19	2.54	2.45
Pacific			
Unjettied or single jetty	4	3.84	3.88
Two jetties	10	2.80	3.21
All inlets	14	3.10	3.40

Table 4

Number of Inlets with W/R Ratio Within Stated Range

Coast/Type of Inlet	Range of W/R: 1 to 100	101 to 200	201 to 300	301 to 500	>500	Average W/R
Atlantic						
Unjettied or single jetty	9	5	10	5	7	337
Two jetties	14	1	1	0	0	67
All inlets	23	6	11	5	7	254
Gulf						
All inlets	8	7	2	0	4	243
Pacific						
Unjettied or single jetty	4	1	0	0	1	272
Two jetties	9	2	0	1	0	90
All inlets	13	3	0	1	1	157

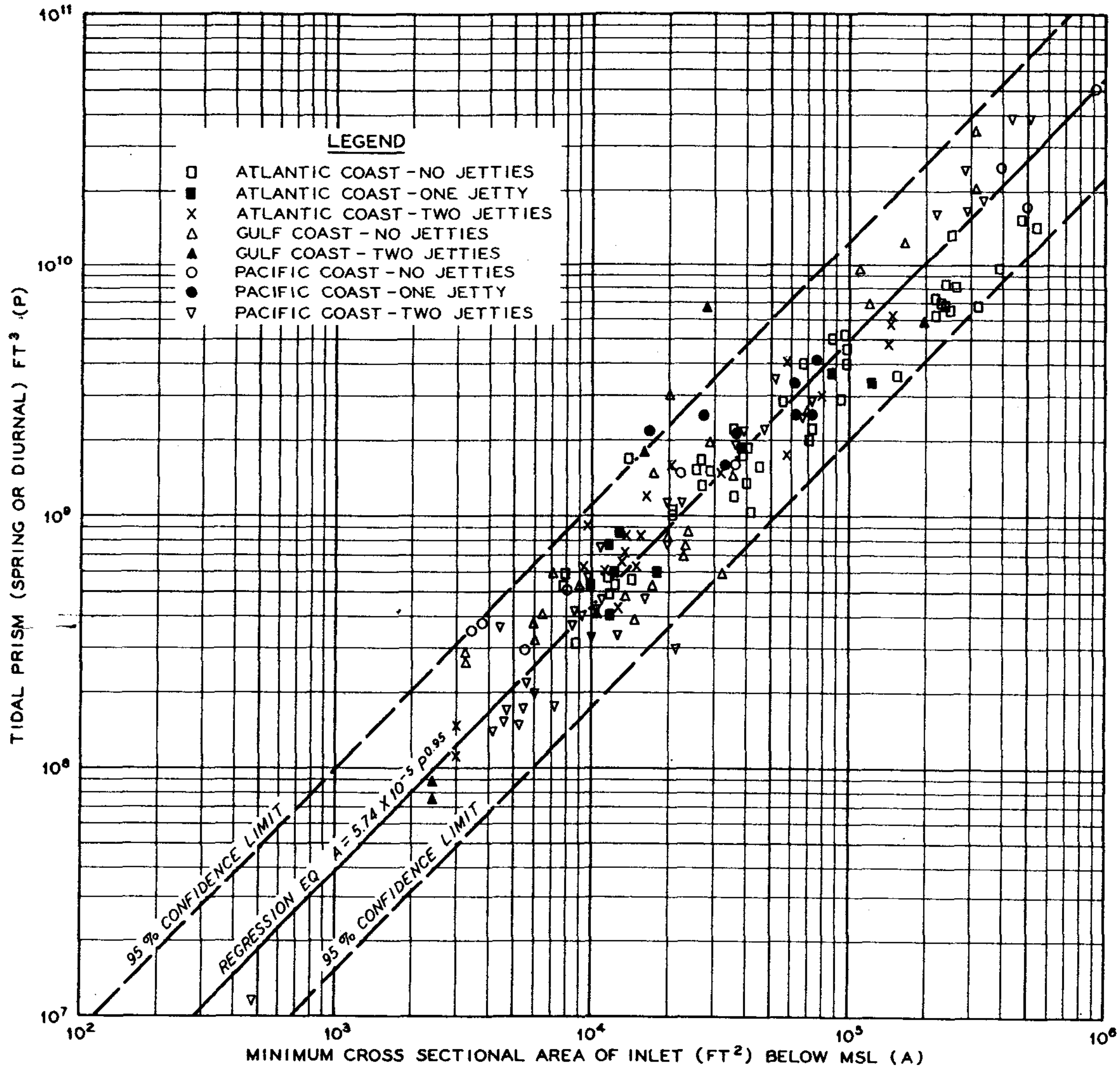

NOTE: REGRESSION CURVE WITH 95 PERCENT CONFIDENCE LIMITS.

TIDAL PRISM VS CROSS-SECTIONAL AREA

ALL INLETS ON ATLANTIC, GULF, AND PACIFIC COASTS

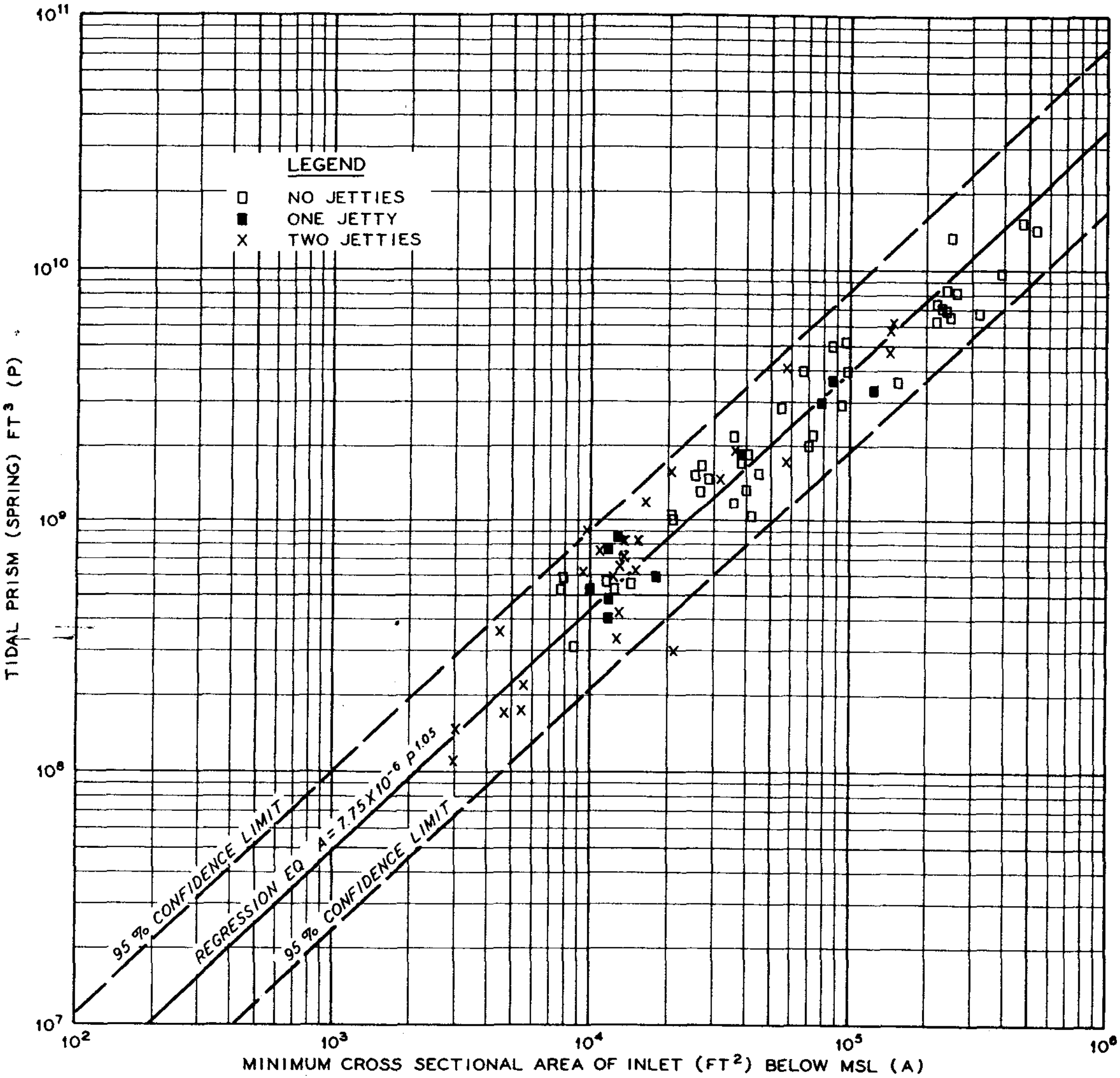

NOTE: REGRESSION CURVE WITH 95 PERCENT CONFIDENCE LIMITS.

TIDAL PRISM VS CROSS-SECTIONAL AREA

ALL INLETS ON ATLANTIC COAST

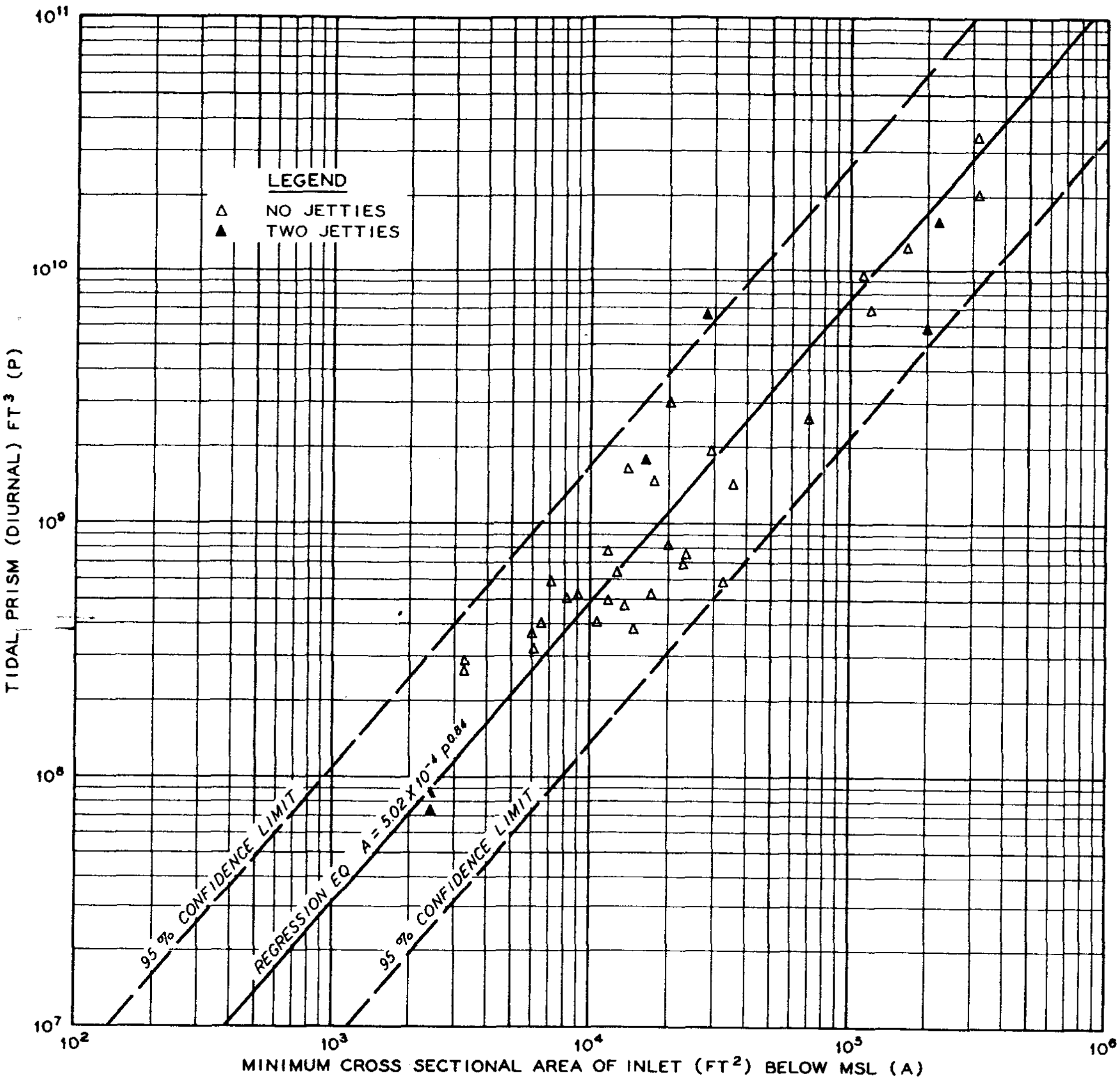

NOTE: REGRESSION CURVE WITH 95 PERCENT CONFIDENCE LIMITS.

TIDAL PRISM VS CROSS-SECTIONAL AREA
ALL INLETS ON GULF COAST

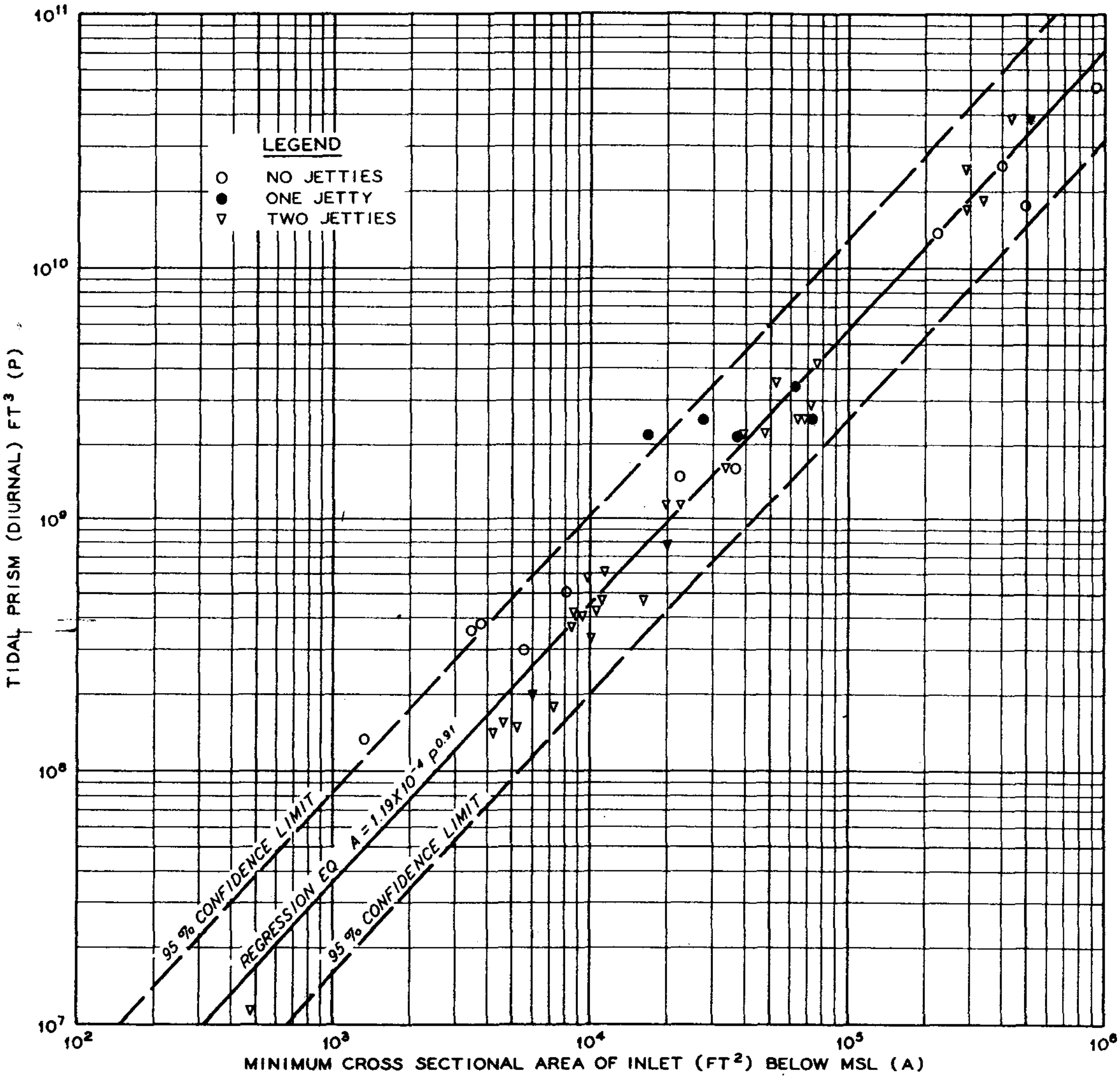

NOTE: REGRESSION CURVE WITH 95 PERCENT CONFIDENCE LIMITS.

TIDAL PRISM VS CROSS-SECTIONAL AREA

ALL INLETS ON PACIFIC COAST

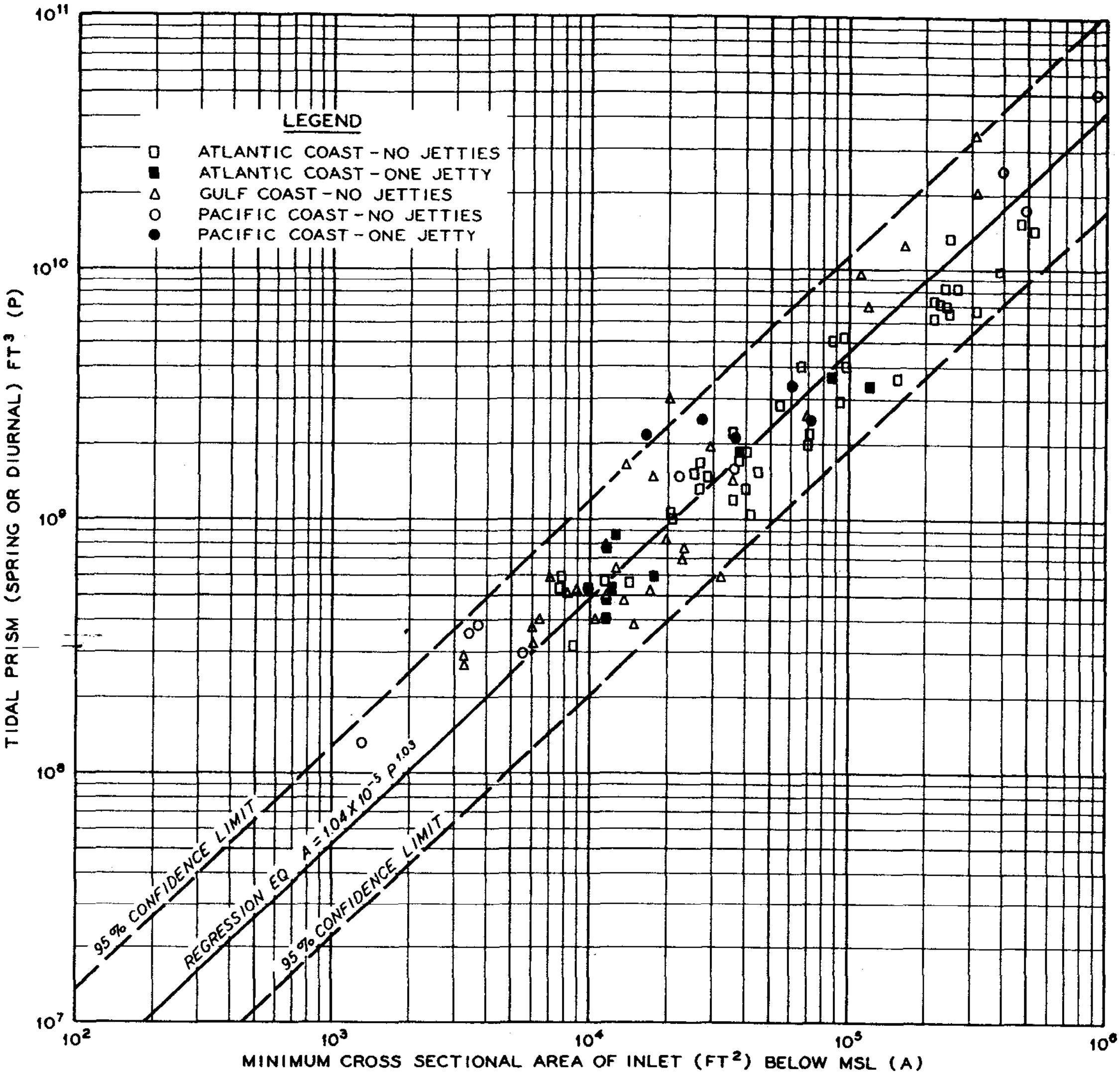

NOTE: REGRESSION CURVE WITH 95 PERCENT CONFIDENCE LIMITS.

TIDAL PRISM VS CROSS-SECTIONAL AREA

INLETS ON ATLANTIC, GULF, AND PACIFIC COASTS WITH ONE OR NO JETTIES

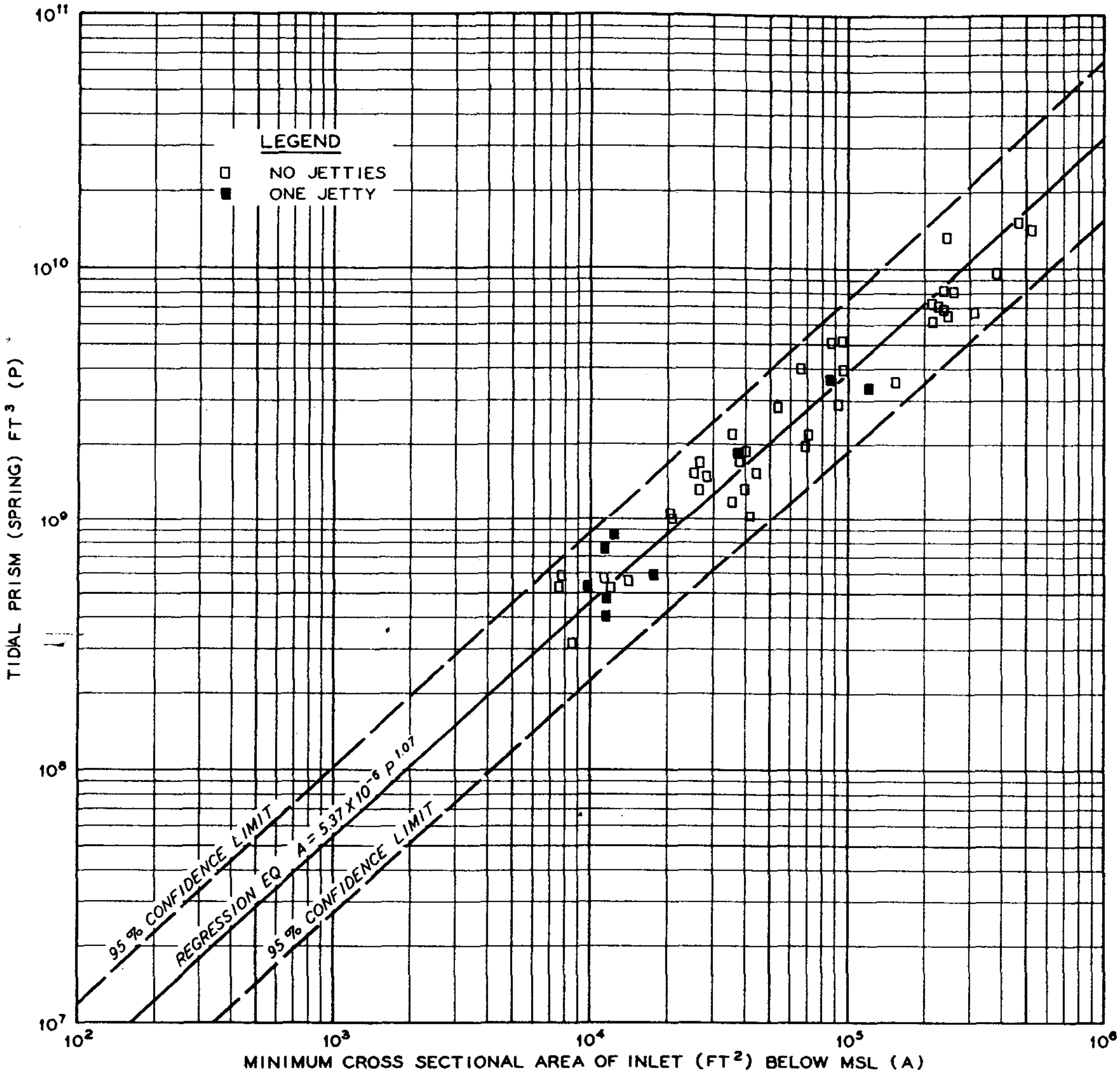

NOTE: REGRESSION CURVE WITH 95 PERCENT CONFIDENCE LIMITS.

TIDAL PRISM VS CROSS-SECTIONAL AREA

INLETS ON ATLANTIC COAST WITH ONE OR NO JETTIES

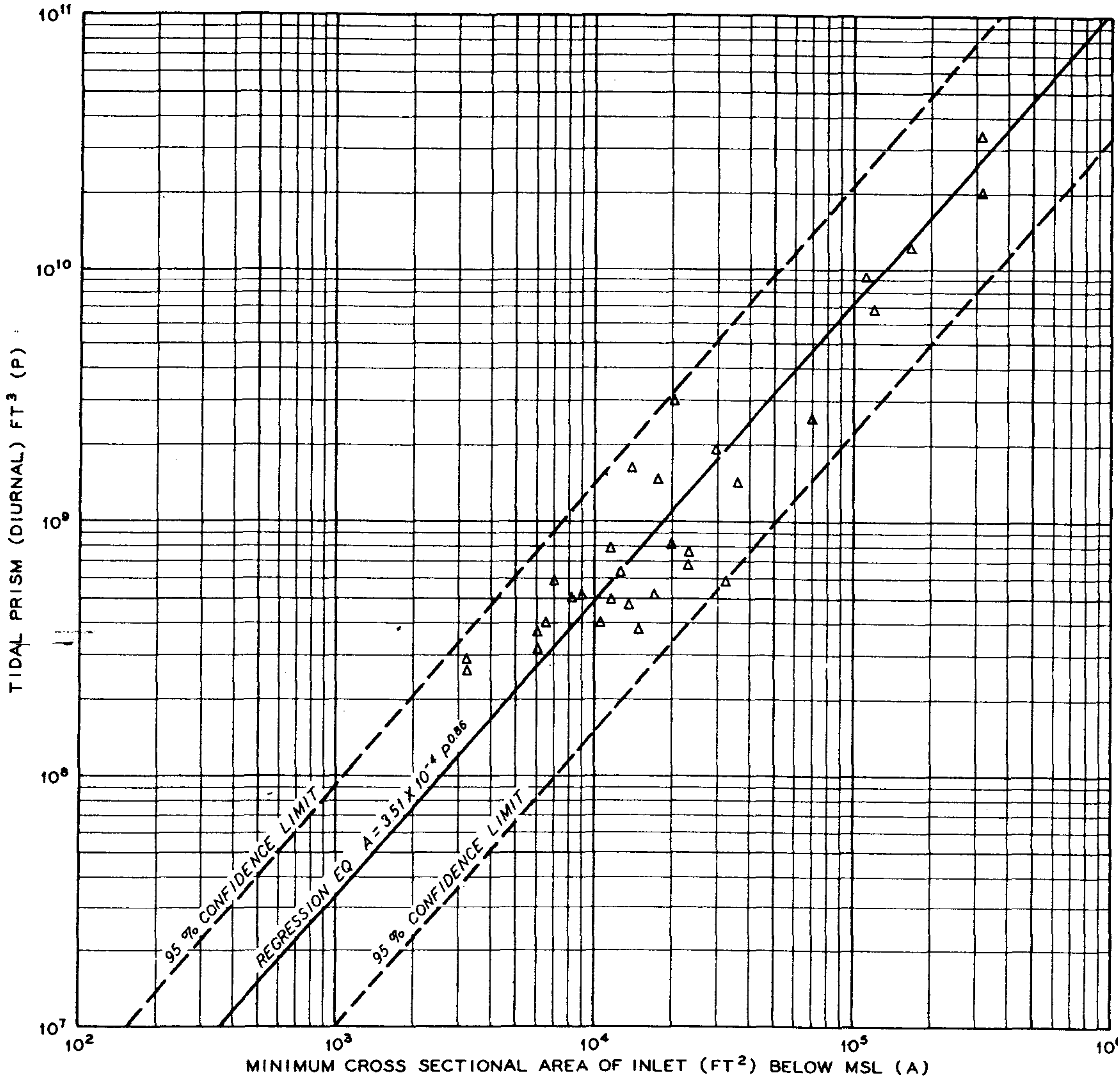

NOTE: REGRESSION CURVE WITH 95 PERCENT CONFIDENCE LIMITS.

TIDAL PRISM VS CROSS-SECTIONAL AREA

INLETS ON GULF COAST WITHOUT JETTIES

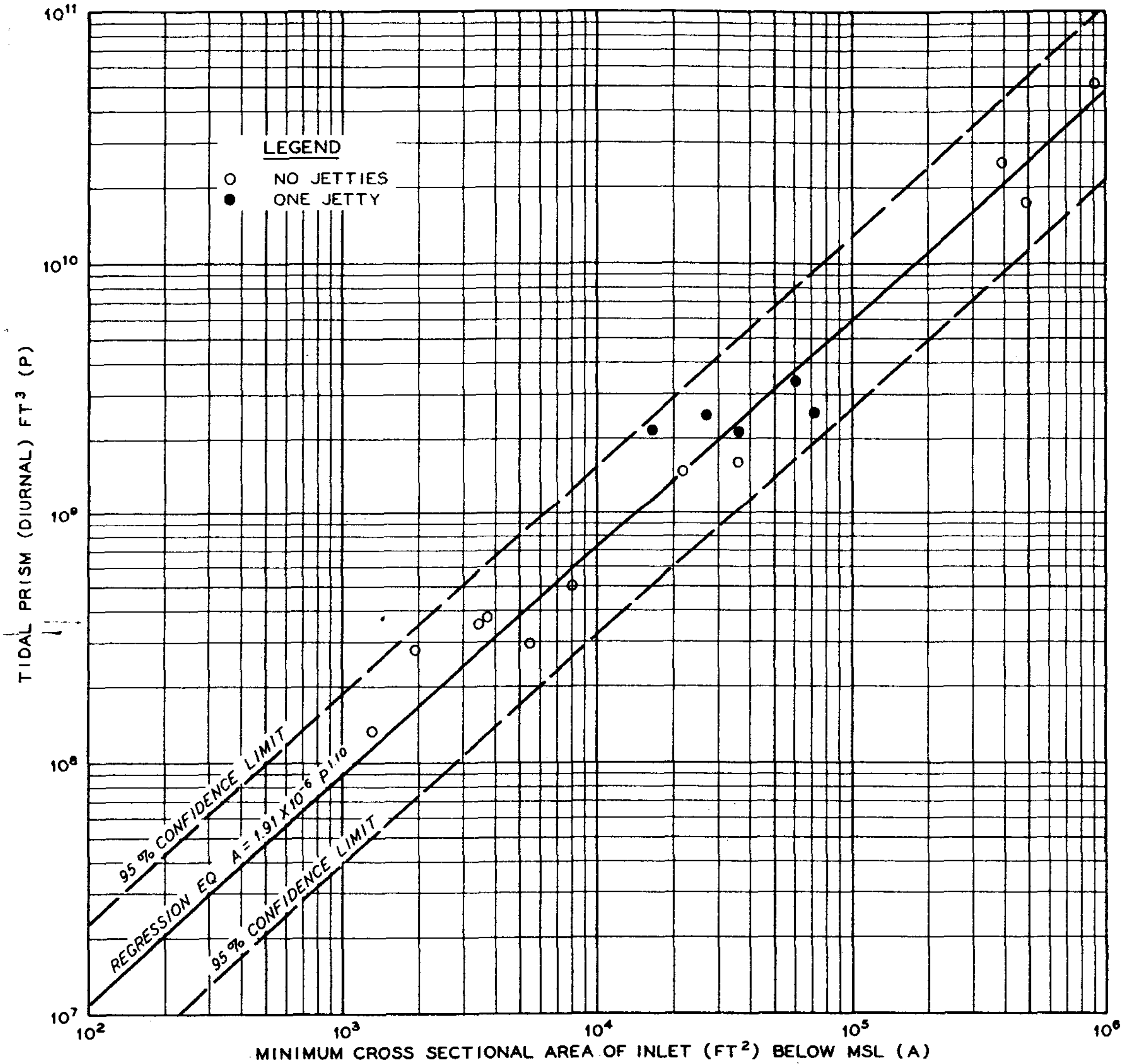

NOTE: REGRESSION CURVE WITH 95 PERCENT CONFIDENCE LIMITS.

TIDAL PRISM VS CROSS-SECTIONAL AREA

INLETS ON PACIFIC COAST WITH ONE OR NO JETTIES

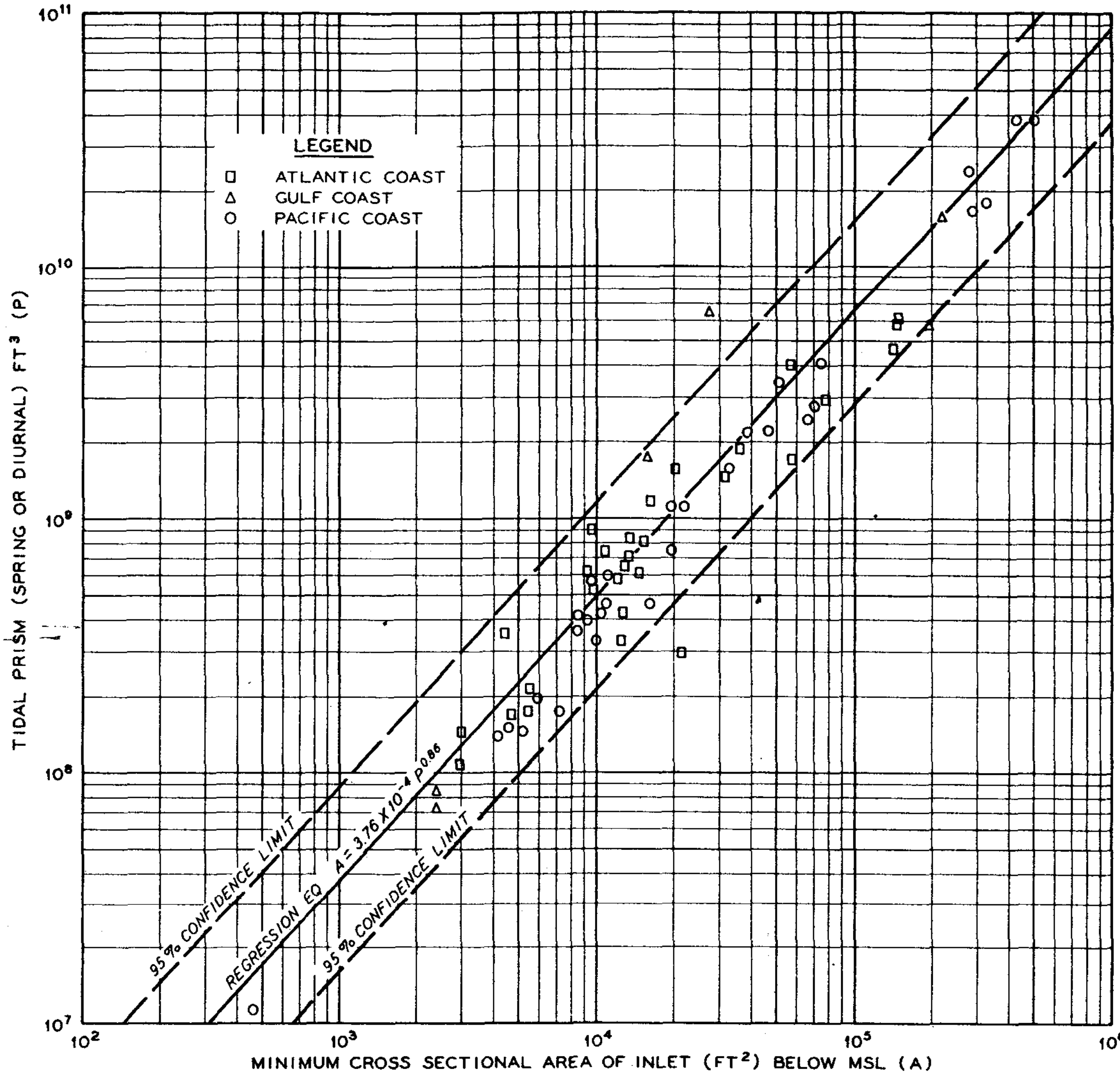

NOTE: REGRESSION CURVE WITH 95 PERCENT CONFIDENCE LIMITS.

TIDAL PRISM VS CROSS-SECTIONAL AREA

INLETS ON ATLANTIC, GULF, AND PACIFIC COASTS WITH TWO JETTIES

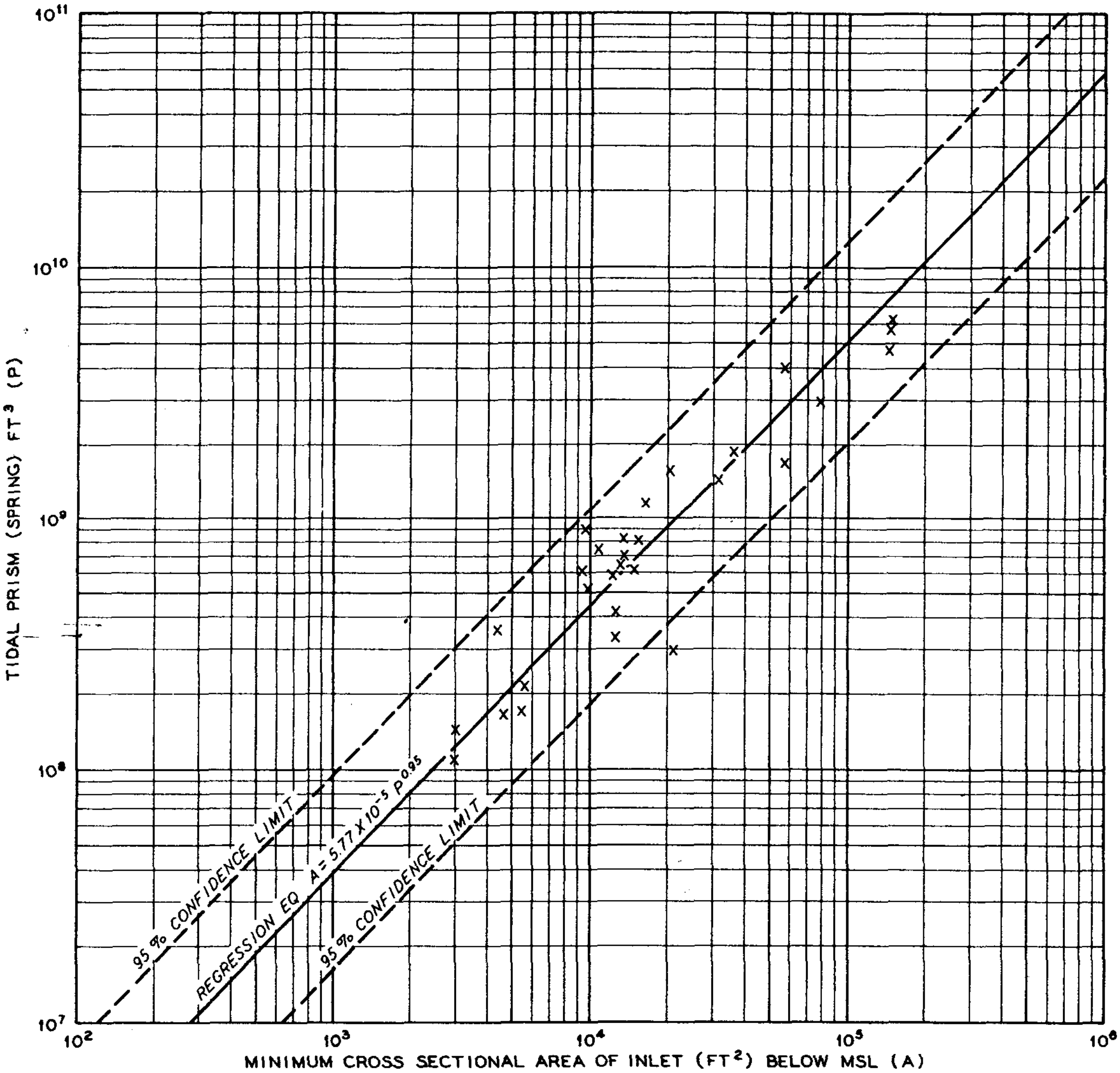

NOTE: REGRESSION CURVE WITH 95 PERCENT CONFIDENCE LIMITS.

TIDAL PRISM VS CROSS-SECTIONAL AREA

INLETS ON ATLANTIC COAST WITH TWO JETTIES

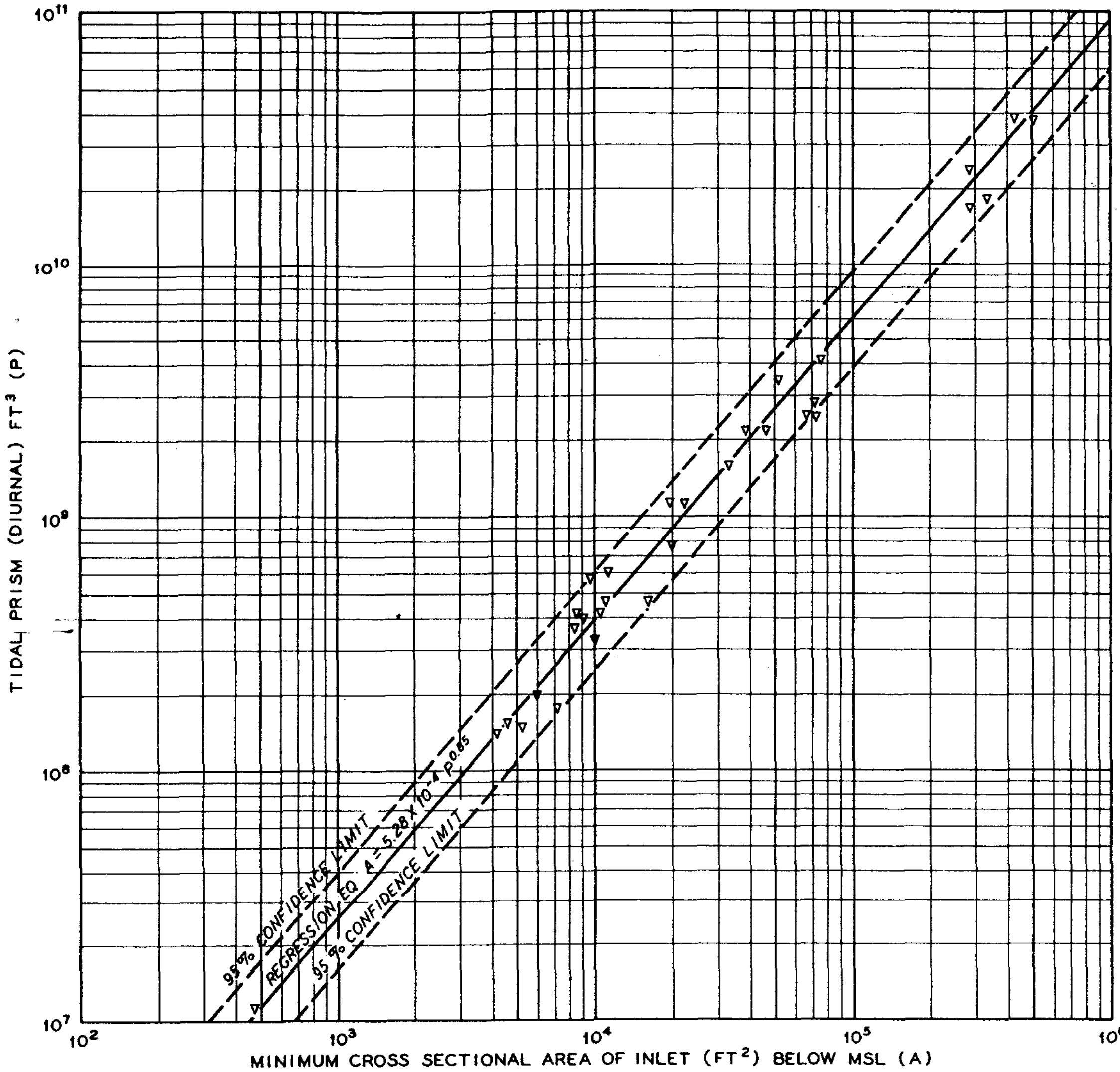

NOTE: REGRESSION CURVE WITH 95 PERCENT CONFIDENCE LIMITS.

TIDAL PRISM VS CROSS-SECTIONAL AREA

INLETS ON PACIFIC COAST WITH TWO JETTIES

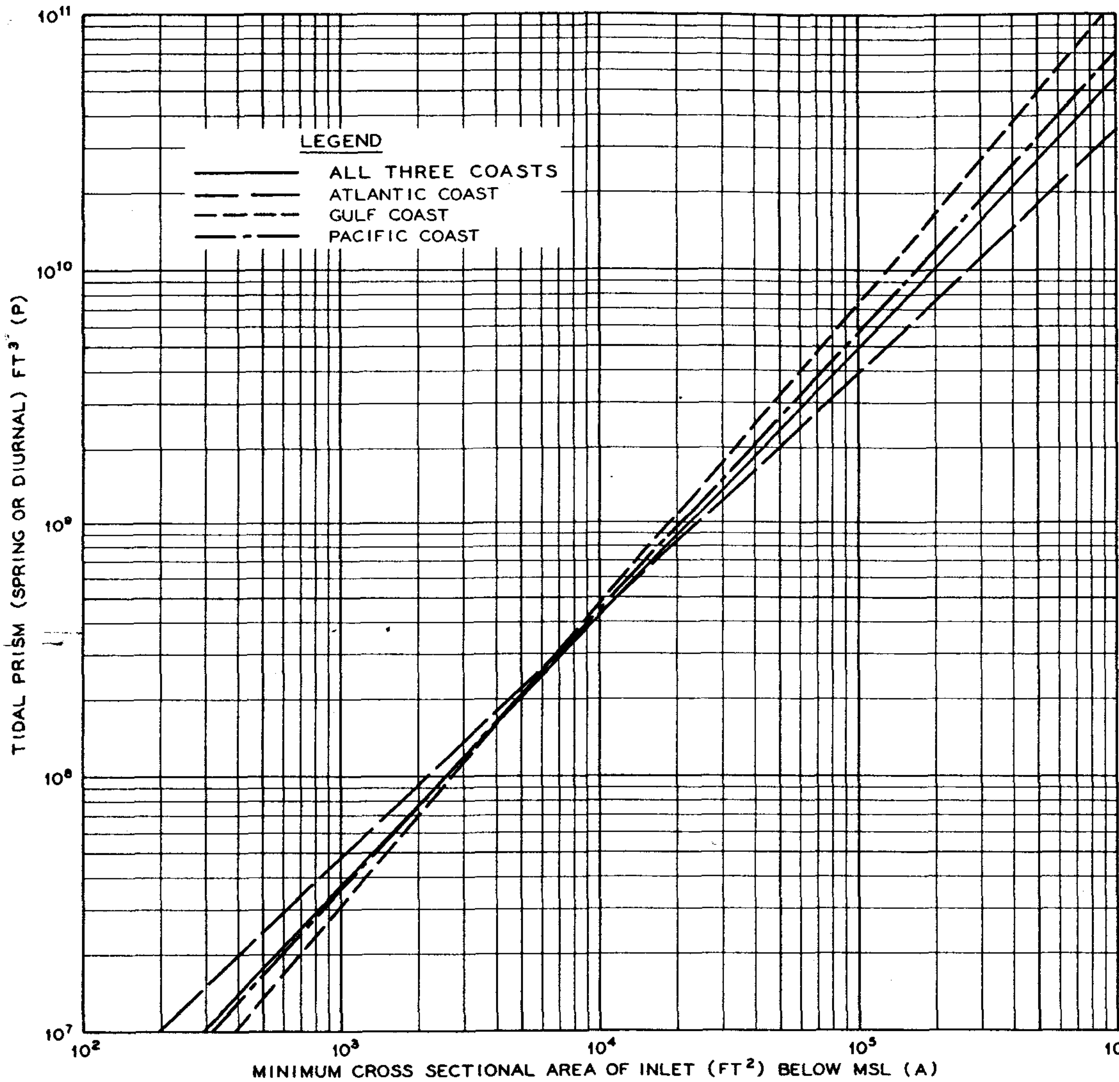

TIDAL PRISM VS
CROSS-SECTIONAL AREA
REGRESSION CURVES FOR ALL INLETS

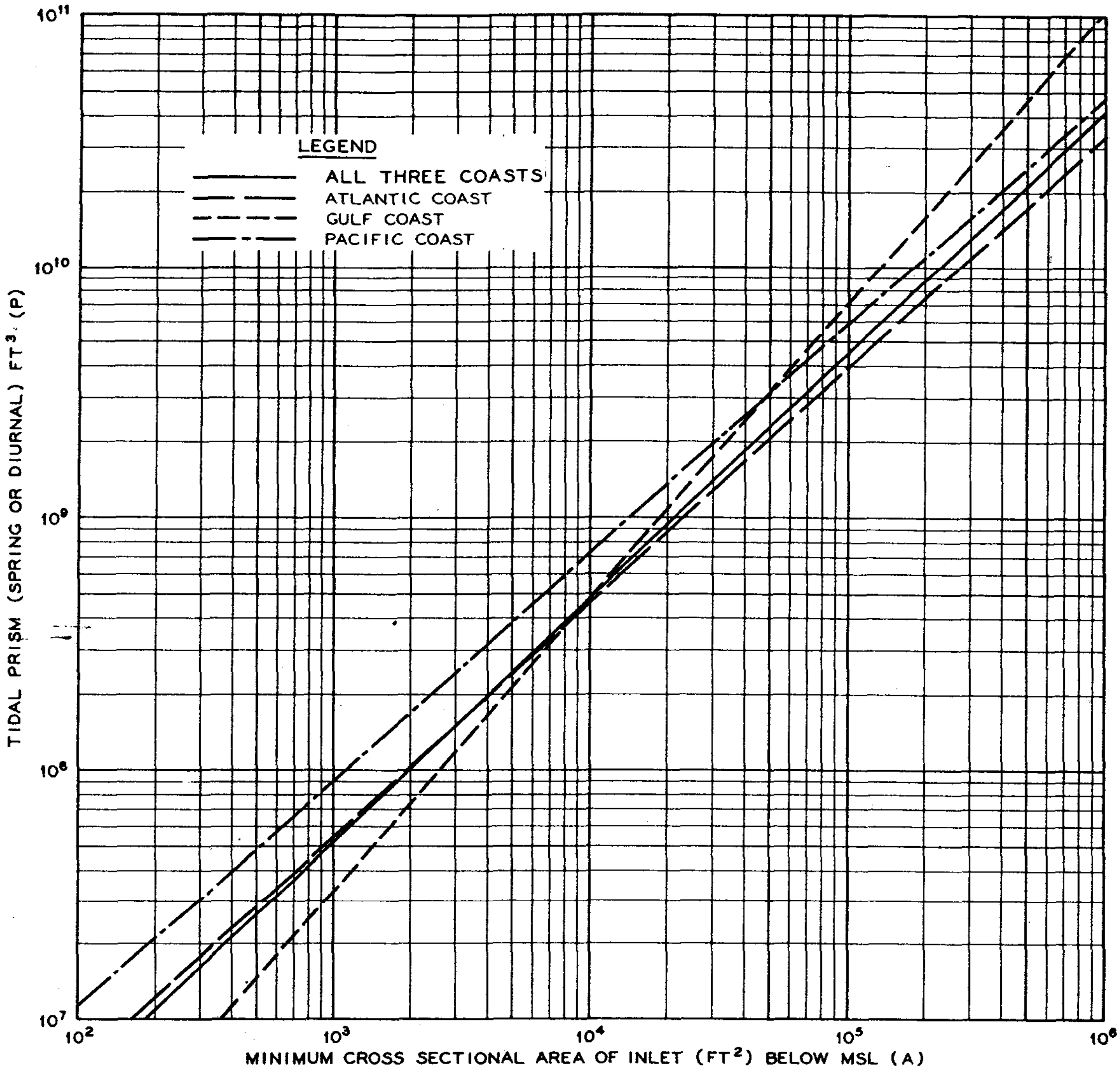

TIDAL PRISM VS
CROSS-SECTIONAL AREA
REGRESSION CURVES FOR INLETS
WITH ONE OR NO JETTIES

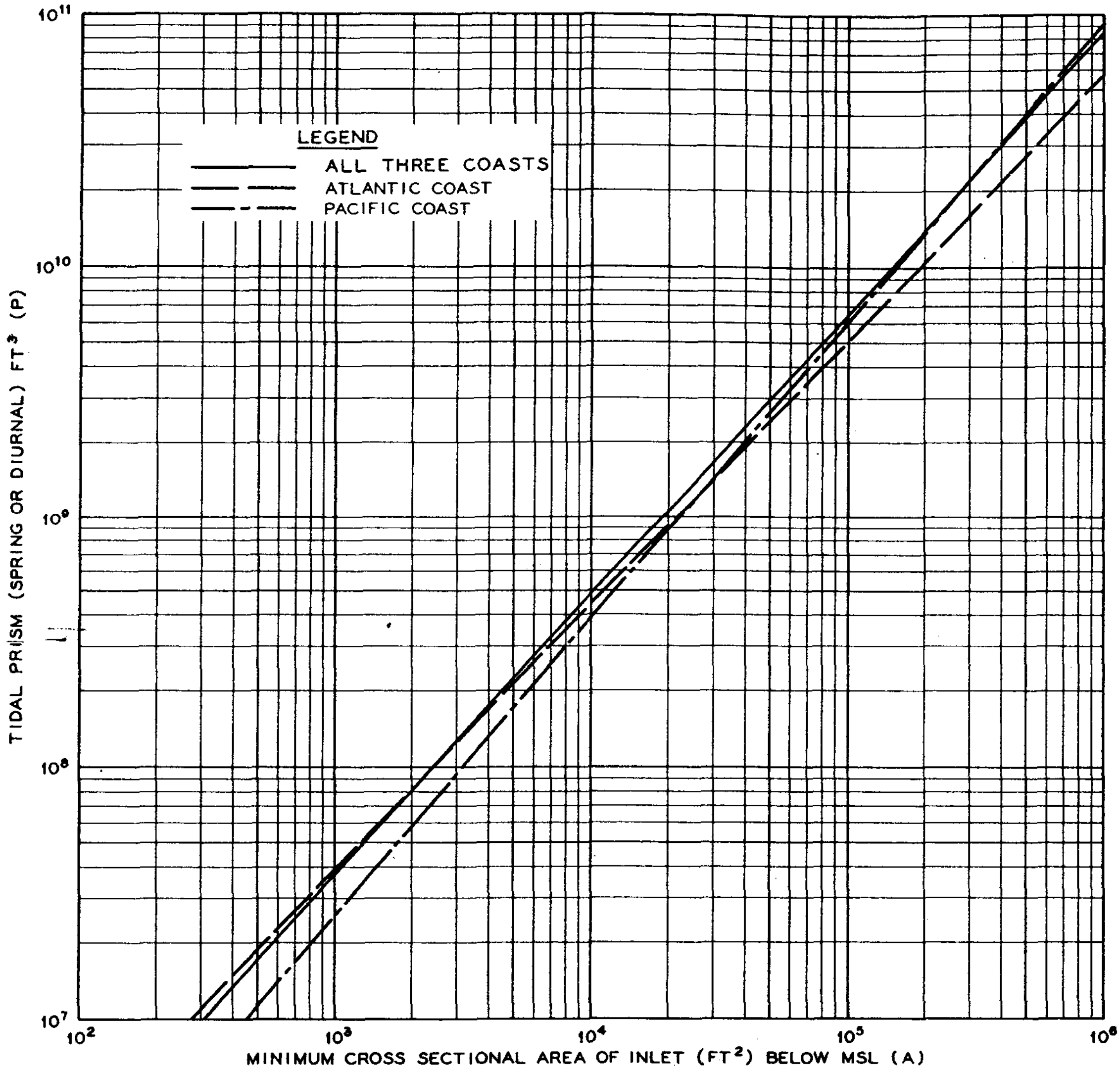

TIDAL PRISM VS CROSS-SECTIONAL AREA

REGRESSION CURVES FOR INLETS WITH TWO JETTIES

APPENDIX A: NOTATION

A	Minimum cross section of the entrance channel measured below msl, sq ft; gorge cross-sectional area below msl, sq ft
C	Regression constant
D	Depth of water at the current meter location, ft
n	Friction coefficient, regression constant
P	Tidal prism corresponding to the diurnal or spring range of tide, cu ft
P_m	Mean tidal prism, cu ft
R	Hydraulic radius at mean sea level, ft
R_1, R_2	Hydraulic radii of Sections 1 and 2, respectively, ft
S_e	Energy gradient
V	Velocity, fps
V_{avg}	Average velocity measured over entire cross section, fps
V_{meas}	Observed velocity at the one vertical section, fps
V_1, V_2	Velocities associated with flow segments 1 and 2, fps
$V_{1_{avg}}, V_{2_{avg}}$	Average velocities through Sections 1 and 2, respectively, fps
W	Width of inlet at mean sea level, ft

In accordance with ER 70-2-3, paragraph 6c(1)(b), dated 15 February 1973, a facsimile catalog card in Library of Congress format is reproduced below.

Jarrett, James T
Tidal prism - inlet area relationships, by James T. Jarrett. Vicksburg, Miss., U. S. Army Engineer Waterways Experiment Station, 1976.
1 v. (various pagings) illus. 27 cm. (U. S. Army. Corps of Engineers. GITI report 3)
General investigation of tidal inlets; a program of research conducted jointly by U. S. Army Coastal Engineering Research Center, Fort Belvoir, Virginia [and] U. S. Army Engineer Waterways Experiment Station, Vicksburg, Mississippi.
Includes bibliography.

1. Tidal inlets. 2. Tidal prisms. I. U. S. Coastal Engineering Research Center. II. U. S. Waterways Experiment Station, Vicksburg, Miss. (Series: U. S. Army. Corps of Engineers. GITI report 3)
GB454.T5.U5 no.3